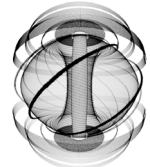


Overview of results from MAST

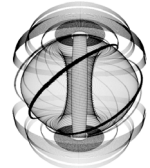
**Presented by:
Glenn Counsell, for the MAST team**

This work was jointly funded by the UK Engineering & Physical Sciences Research Council and Euratom

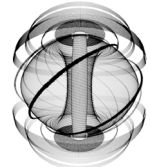


Focus on 4 areas

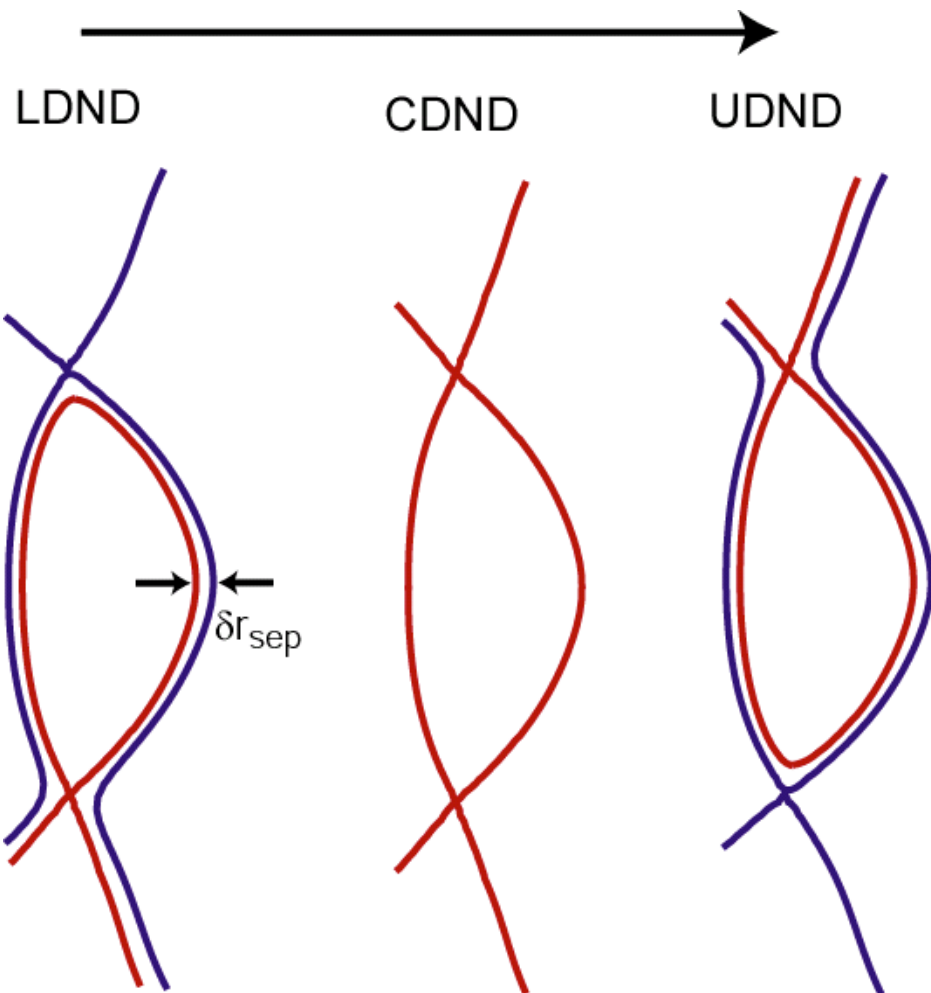
- The L-H transition and H-mode Pedestal
- Confinement and Transport
- Transients - ELMs and Disruptions
- Start-up without a central solenoid



-
- The L-H transition and H-mode Pedestal
 - Confinement and Transport
 - Transients - ELMs and Disruptions
 - Start-up without a central solenoid



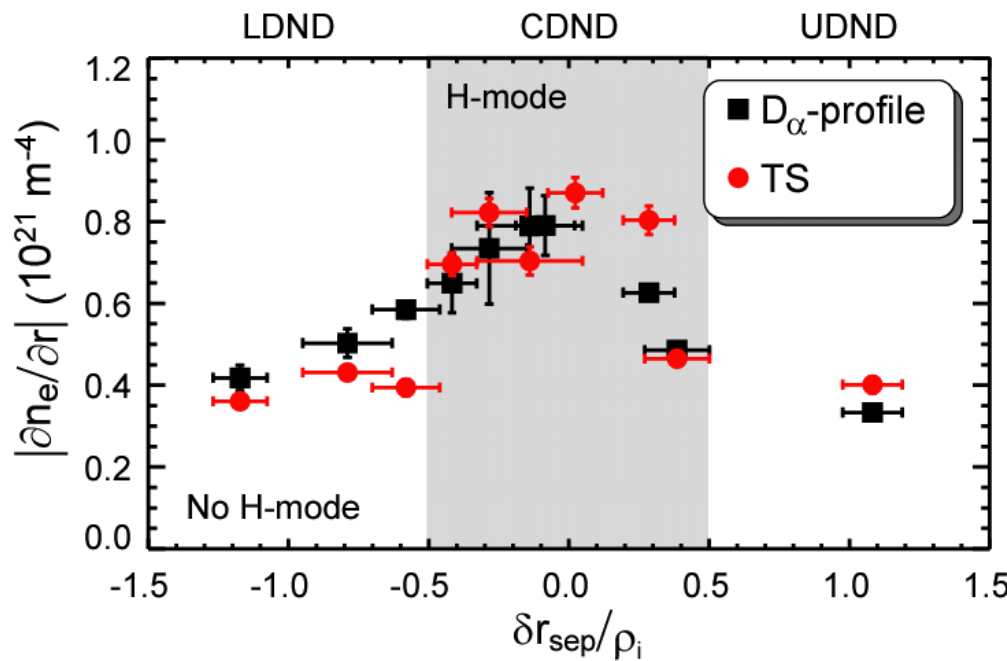
δr_{sep} plays a key role in MAST



MAST has fully symmetric upper and lower divertors and can operate from LSN to USN



CDND lowers P_{L-H}



MAST has fully symmetric upper and lower divertors and can operate from LSN to USN

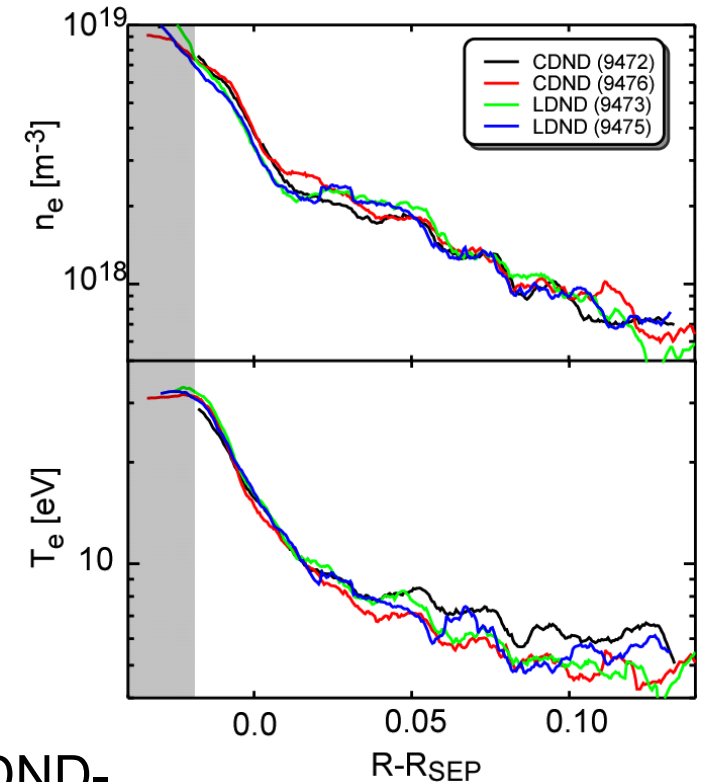
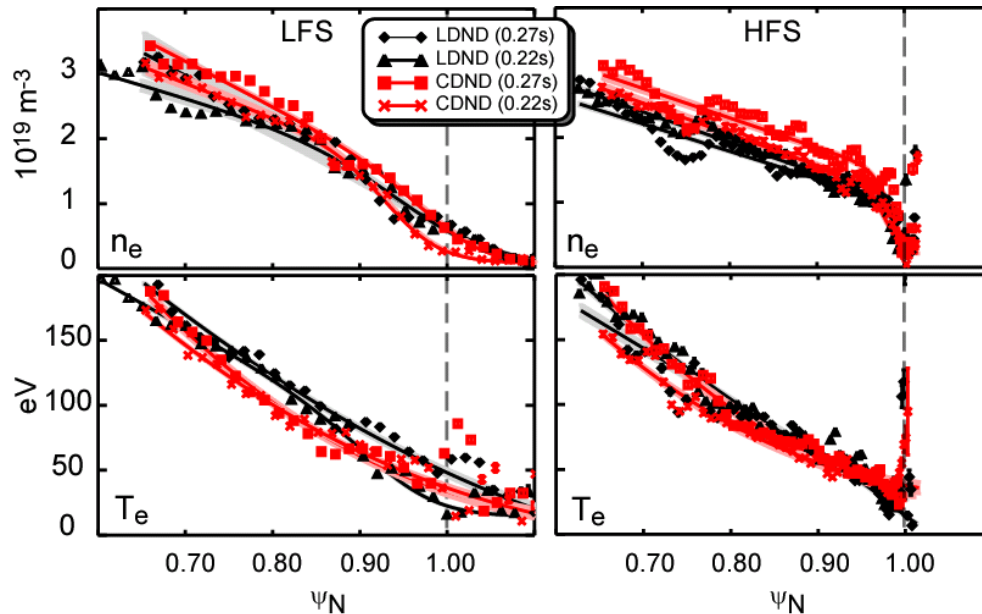
Previously reported that H-mode difficult to obtain on MAST away from Connected DND

New studies now show that P_{L-H} decreases by factor 2 in CDND compared to similar shaped Lower SND plasmas

Same trend observed in MAST-
ASDEX upgrade similarity experiments. **Factor 1.25 reduction in P_{L-H}**



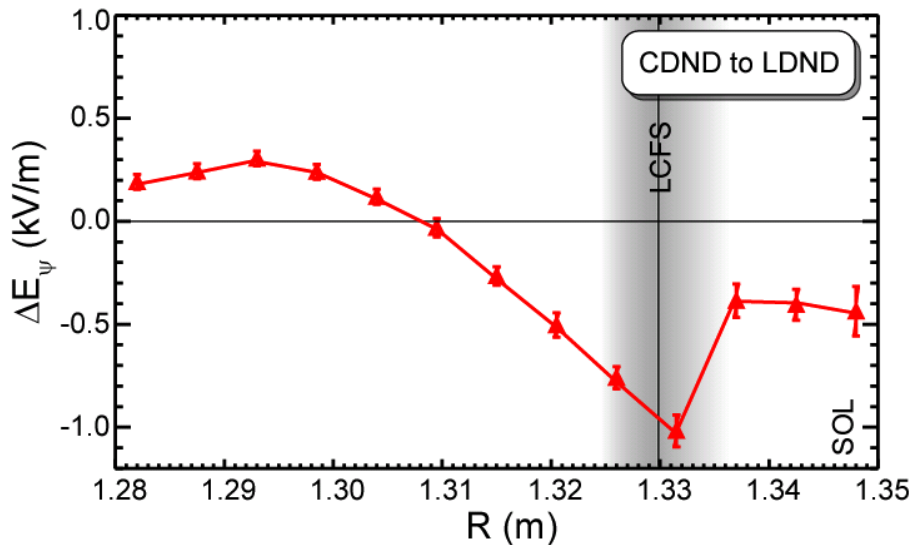
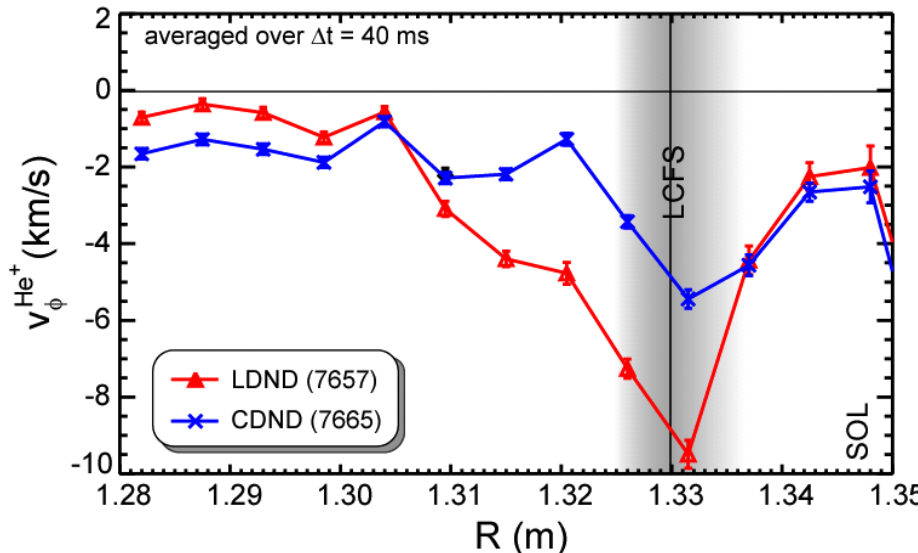
No significant changes to edge profiles



In L-mode (close to P_{L-H}) change from LSND-LDND-CDND **not evident in edge T_e , n_e , V_f and M_ϕ profiles**



Only V_ϕ and E_r influenced by CDND



In L-mode (close to P_{L-H}) change from LSND-LDND-CDND **not evident in edge T_e , n_e , V_f and M_ϕ profiles**

Only clearly observed on impurity rotation and thus radial electric field

Magnitude of change at LFS separatrix similar to that observed in ASDEX Upgrade similarity experiments



L-H transition models tested

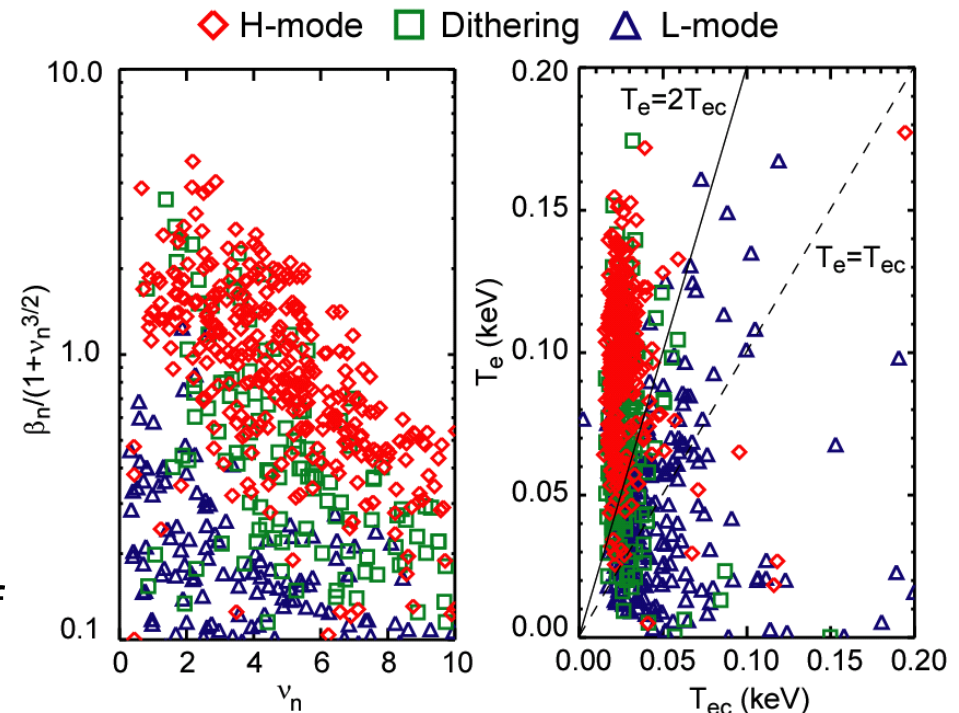
Common theories for L-H transition investigated

Two theories successful in separating L and H-mode data:

Best separation achieved by $\beta_n/(1+v_n^{3/2})$ at ψ_{95} , which characterises **suppression of long λ drift wave turbulence** - but not quantitative.

Best quantitative separation achieved by critical T_e at ψ_{98} from **finite β drift wave turbulence suppression** by self generated zonal flows

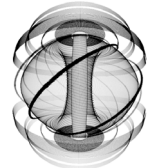
Neither theory accounts explicitly for impact of CDND



W. Kerner et al.

P. Gudzar et al.

See H. Meyer EX/P3-8

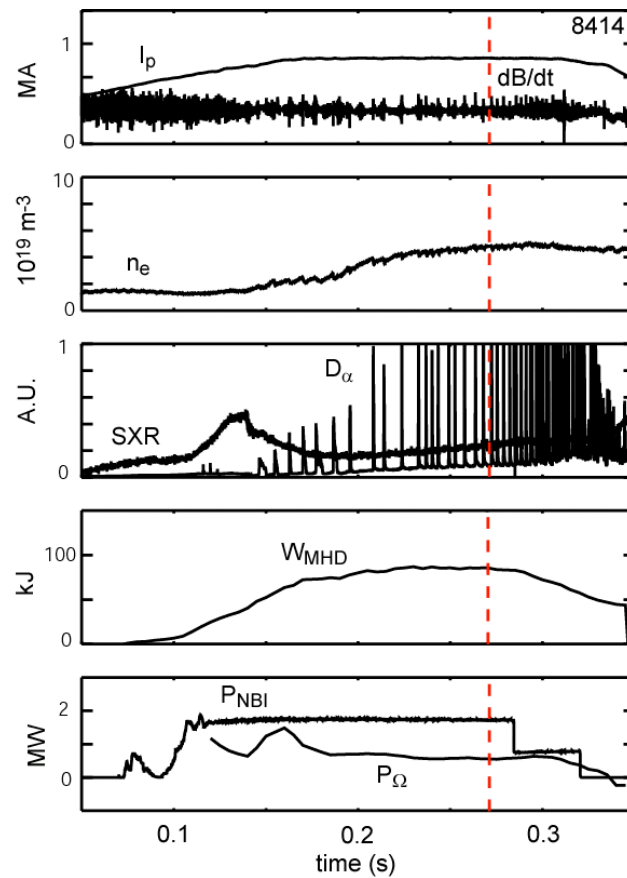


-
- The L-H transition and H-mode Pedestal
 - **Confinement** and Transport
 - Transients - ELMs and Disruptions
 - Start-up without a central solenoid



Confinement data at high β and ϵ

Many new MAST points meeting stringent International Database criteria added to database





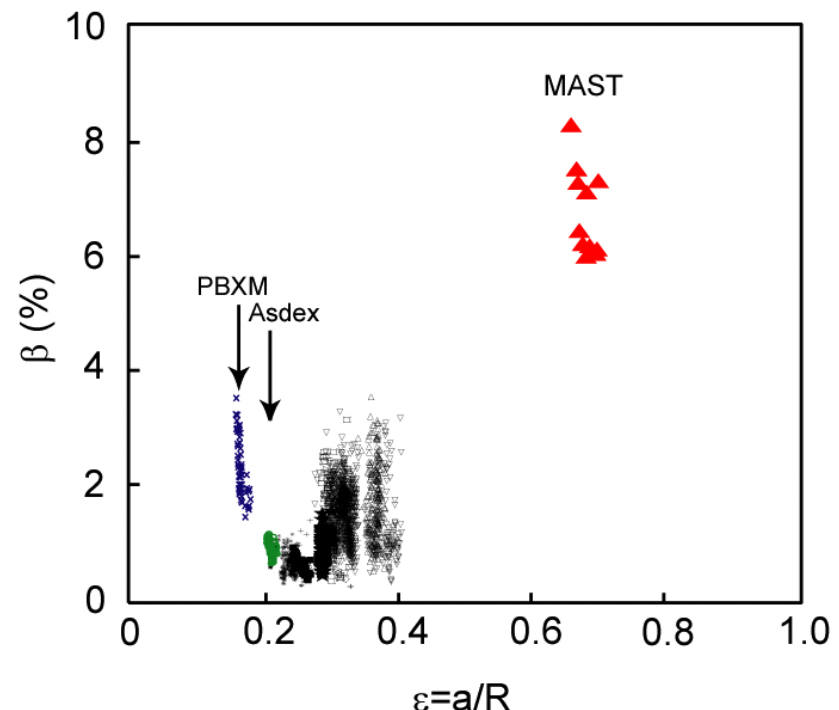
Confinement data at high β and ϵ

Many new MAST points meeting stringent International Database criteria added to database

MAST data expand the range of **inverse aspect ratio ($\epsilon=a/R$) by a factor 2.2** and in **toroidal β by a factor 2.5**

Improve confidence by allowing replacement of data from devices non-conventional cross-sections

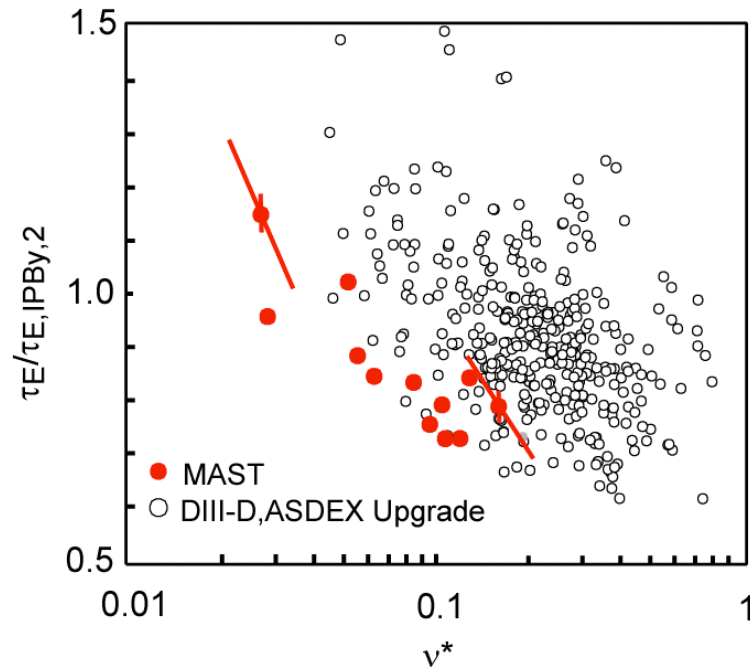
Largely support existing IPB($y,2$) scaling but slightly strengthen ϵ dependance



v^* is a key parameter for ST scalings



MAST data alone support **favourable**
 v^* dependence in dimensionless
parameter scaling



See M. Valovic EX/P6-30

ν^* is a key parameter for ST scalings

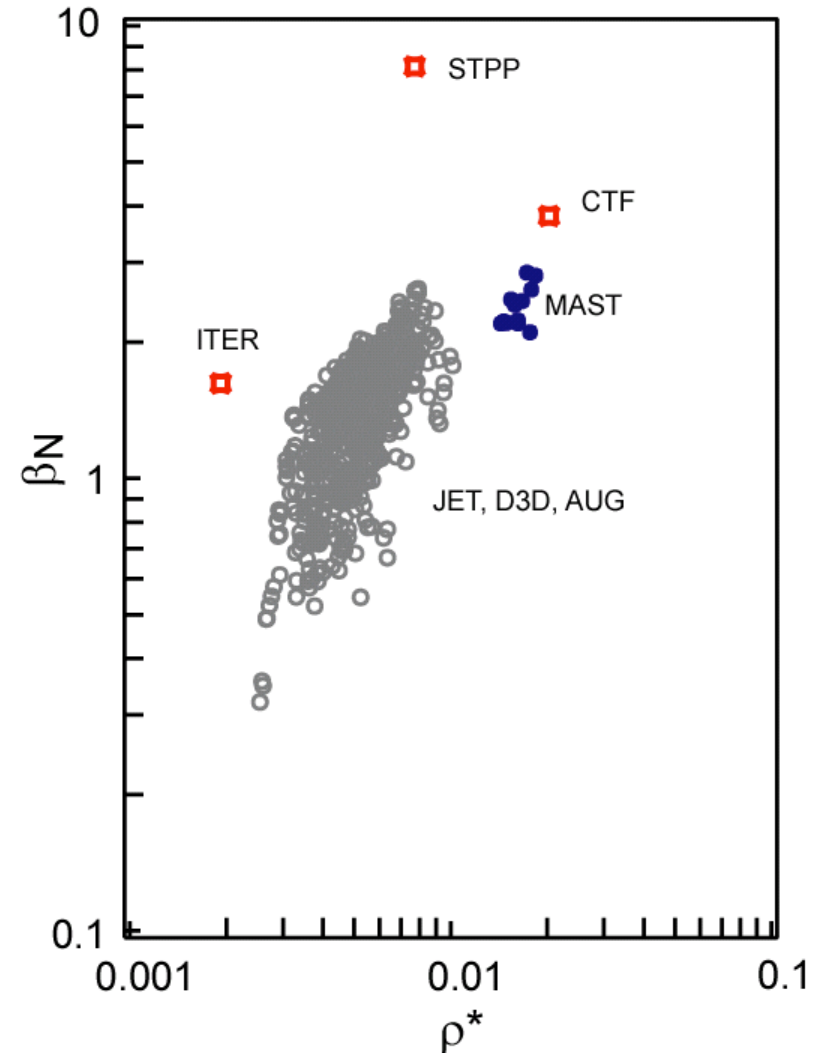


MAST data alone support **favourable ν^* dependence** in dimensionless parameter scaling

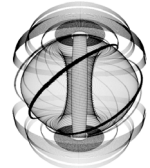
Since β_N and ρ^* in MAST close to possible 'next-generation' ST - understanding ν^* dependence especially important $\nu^{*,\text{MAST}}/\nu^{*,\text{CTF}} \sim 90$

Link between dependencies of β and ε provided by MAST data may be useful

⇒ ε should be included in recently identified interaction between β and ν^* exponents in dimensionless scaling)



See M. Valovic EX/P6-30, H.R. Wilson FT/3-1Ra



-
- The L-H transition and H-mode Pedestal
 - Confinement and **Transport**
 - Transients - ELMs and Disruptions
 - Start-up without a central solenoid

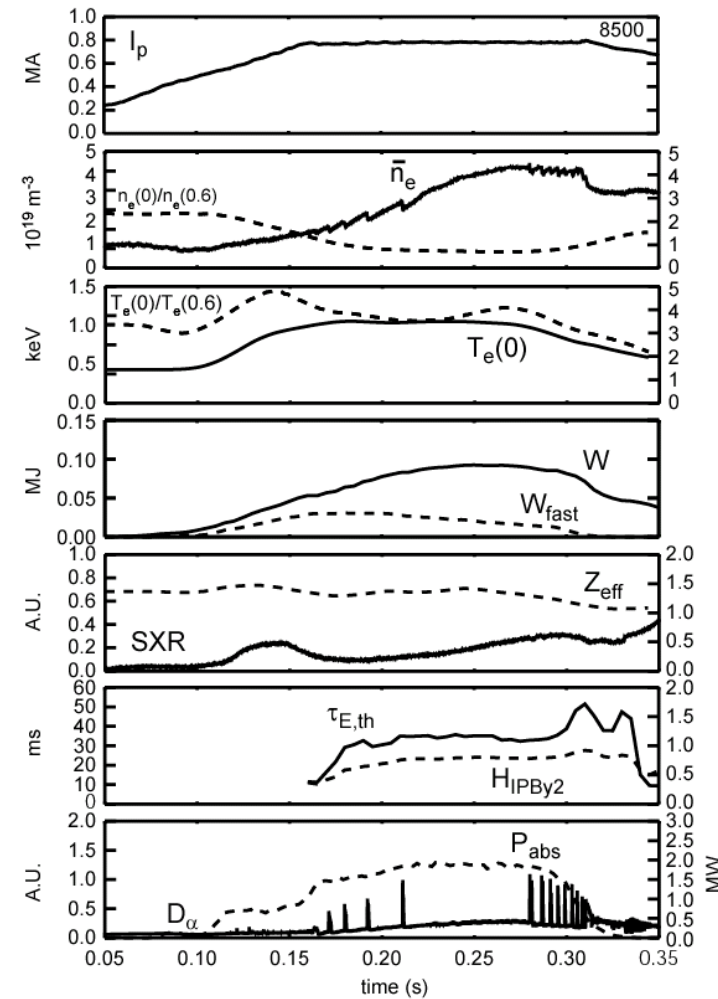


TRANSP analysis now regularly conducted

TRANSP analysis now regularly conducted for MAST discharges

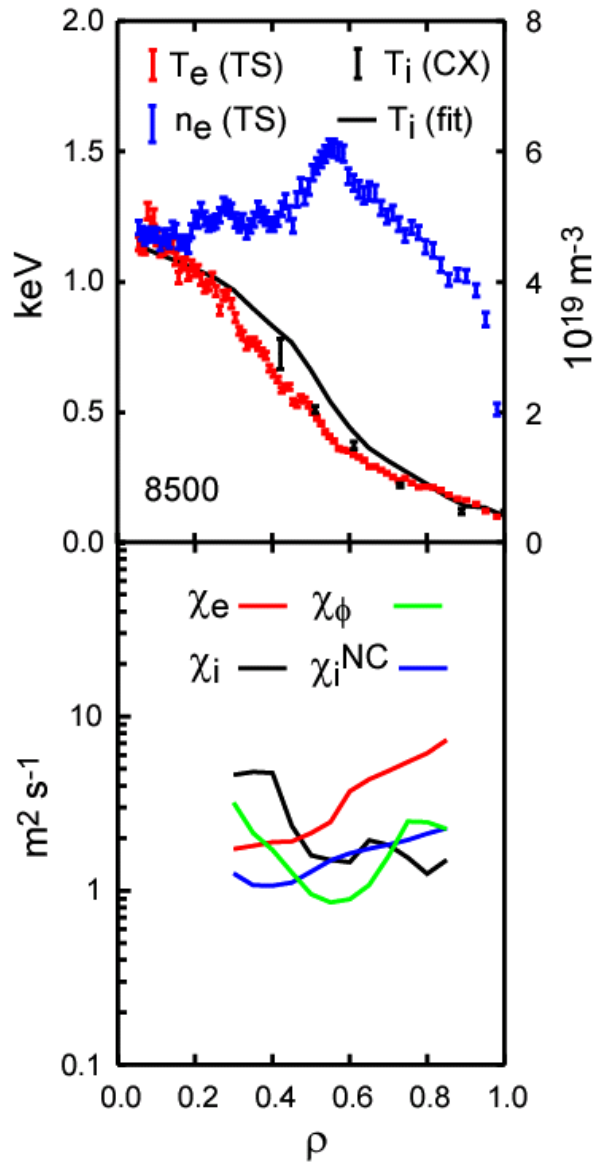
Pre-processor ensures highest quality and greatest range diagnostic data used in analysis

Results validated and cross-checked against LOCUST full-orbit code





TRANSP analysis of ELMy H-mode



Results most accurate in region $0.3 < \rho < 0.8$ (avoiding low gradient regions and larger diagnostic errors)

For $\rho > 0.4$ the ion diffusivity, χ_i is found roughly equal to χ_i^{NC} , cf factor 4 larger in similar L-mode

Linear microstability calcs. using GS2 suggest ITGs unstable on all surfaces:

Mixing length estimates $\Rightarrow \chi_{ITG}^i \sim 3-5 \text{ m}^2 \text{s}^{-1}$, close to TRANSP value

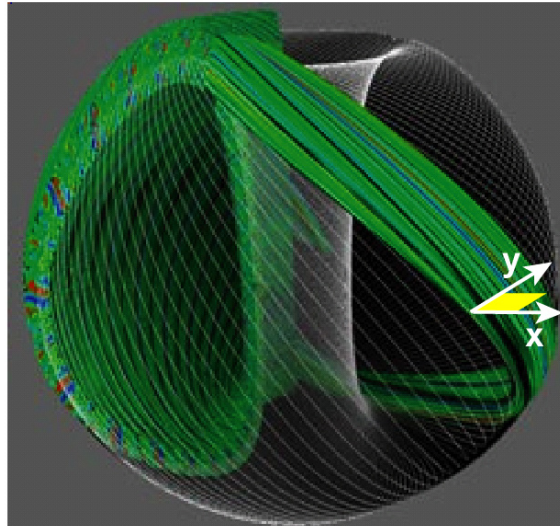
v_ϕ can dominate flow shear ω_{se} \Rightarrow possible ITG drive stabilisation and expect ITBs!

$\chi_{ETG}^e \sim 0.1 \text{ m}^2 \text{s}^{-1}$, far below TRANSP value
 \Rightarrow need for non-linear calcs.

See A.R. Field EX/P2-11



Non-linear GS2 analysis for e⁻ transport



Nonlinear collisionless ETG calculations in flux-tube geometry, assuming adiabatic ions, at $\Psi_n=0.4$ surface in MAST

- base case flux-tube dimensions:
 $\Delta x = 690 \rho_e = 8.7 \text{ cm}$, $\Delta y = 628 \rho_e = 7.9 \text{ cm}$,
 $0.01 < k_y \rho_e < 0.31$

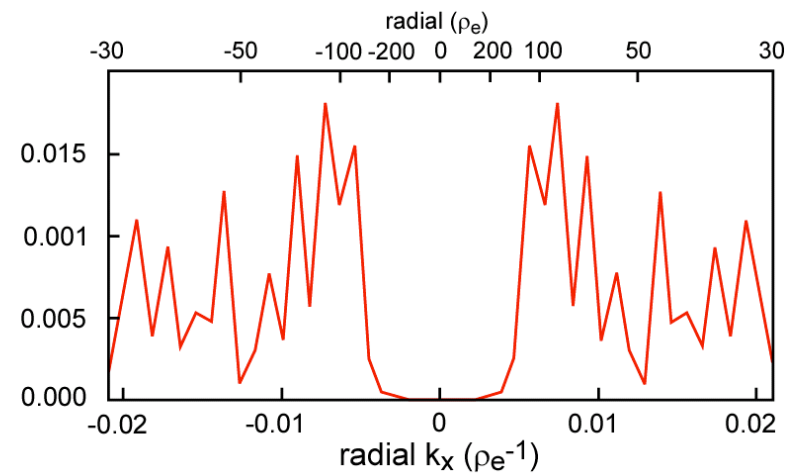
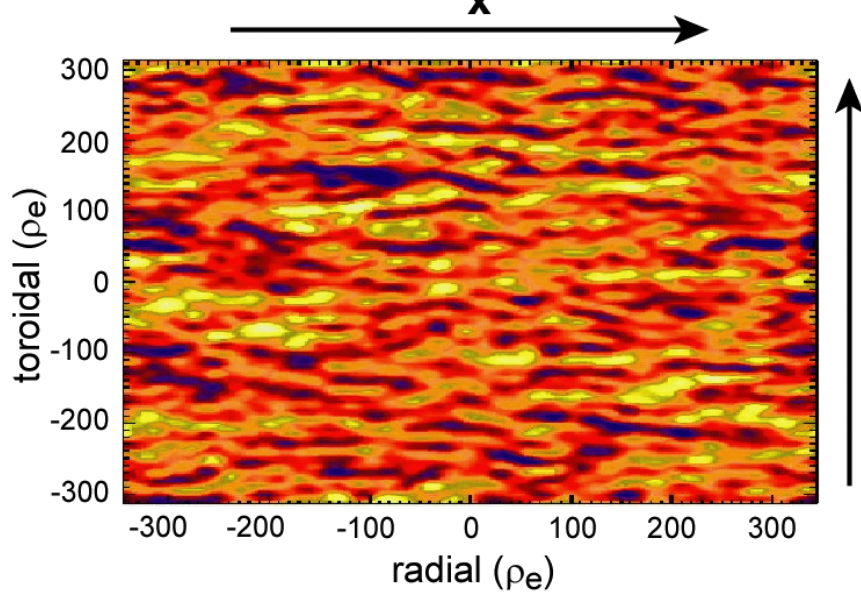


Radial electrostatic streamers predicted

Nonlinear collisionless ETG calculations in flux-tube geometry, assuming adiabatic ions, at $\Psi_n=0.4$ surface in MAST

- base case flux-tube dimensions:
 $\Delta x = 690 \rho_e = 8.7 \text{ cm}$, $\Delta y = 628 \rho_e = 7.9 \text{ cm}$,
 $0.01 < k_y \rho_e < 0.31$

**Radial electrostatic streamers observed
in calculations up $\sim 100 \rho_e$ wide ($\sim 1 \text{ cm}$)**





Converged solution consistent with χ_e

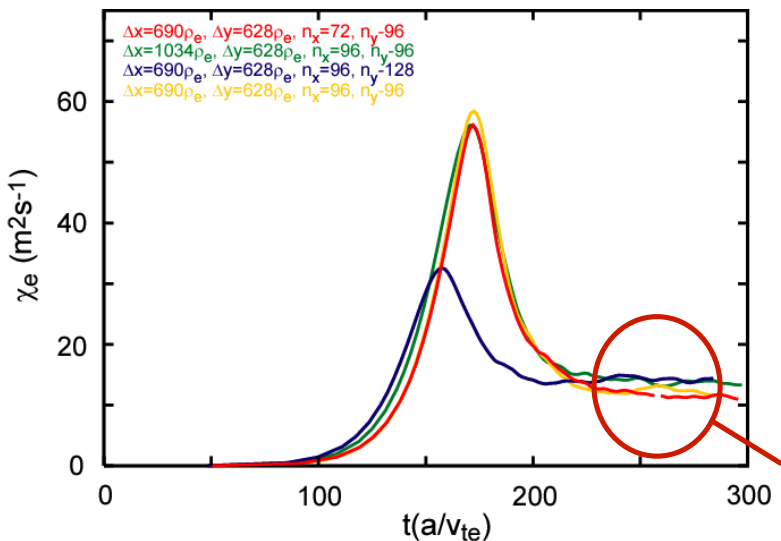
Nonlinear collisionless ETG calculations in flux-tube geometry, assuming adiabatic ions, at $\Psi_n=0.4$ surface in MAST

- base case flux-tube dimensions:
 $\Delta x = 690\rho_e = 8.7\text{cm}$, $\Delta y = 628\rho_e = 7.9\text{cm}$,
 $0.01 < k_y \rho_e < 0.31$

Radial electrostatic streamers observed in calculations up $\sim 100\rho_e$ wide ($\sim 1\text{cm}$)

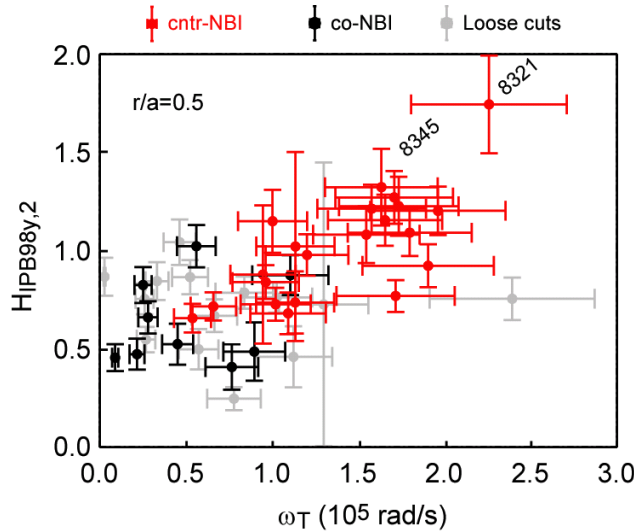
Nonlinear simulation **converges well for range of flux tube dimensions and wavenumbers**

Indicates $\chi_e \sim 10 \text{ m}^2/\text{s}$ (cf Gyro-Bohm estimate of $\chi_e = 0.6 \text{ m}^2/\text{s}$) - **within a factor 2 of TRANSP value**





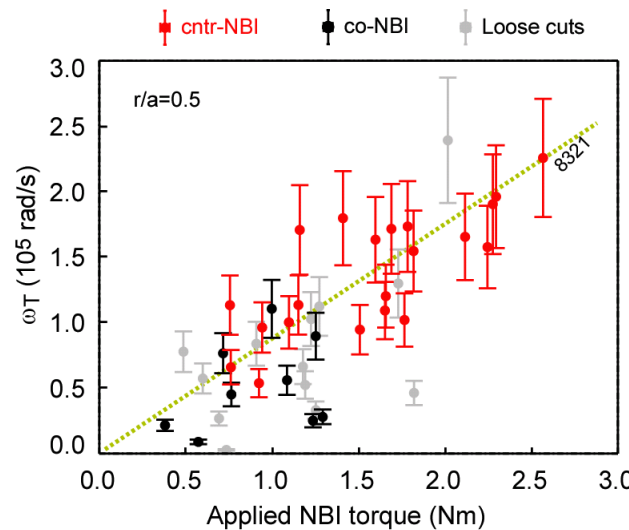
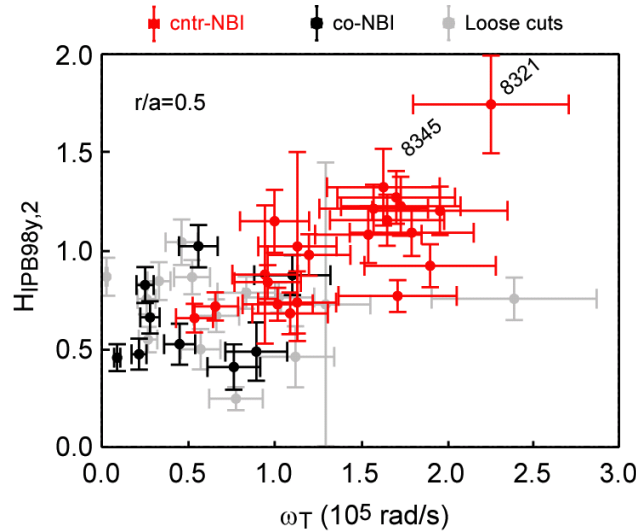
Highest confinement at largest v_ϕ



Normalised confinement
across range of L-mode, H-
mode and ITB discharges
increases with v_ϕ



v_ϕ driven by NBI torque

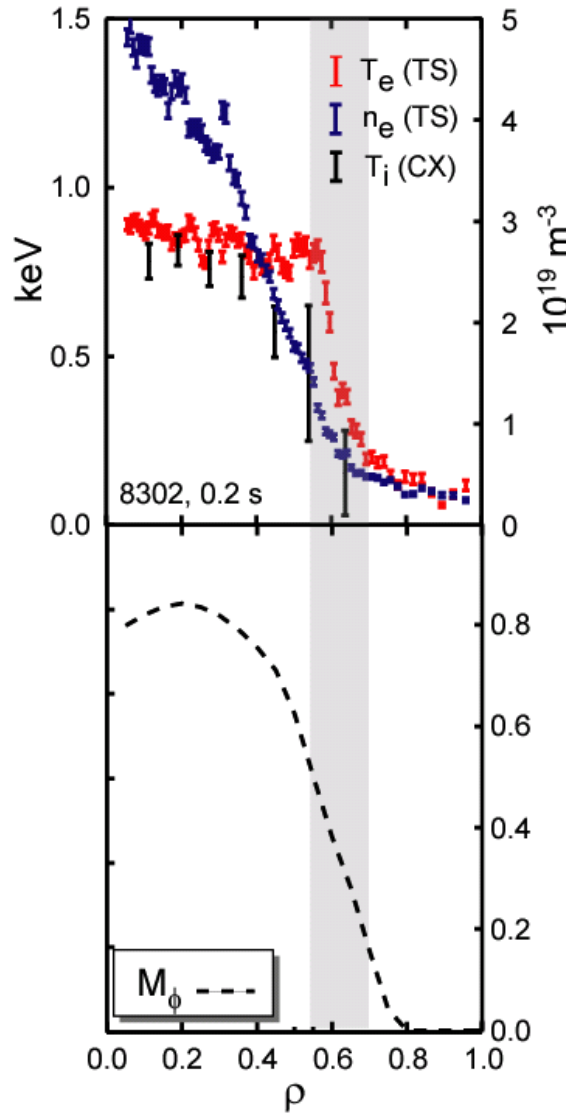
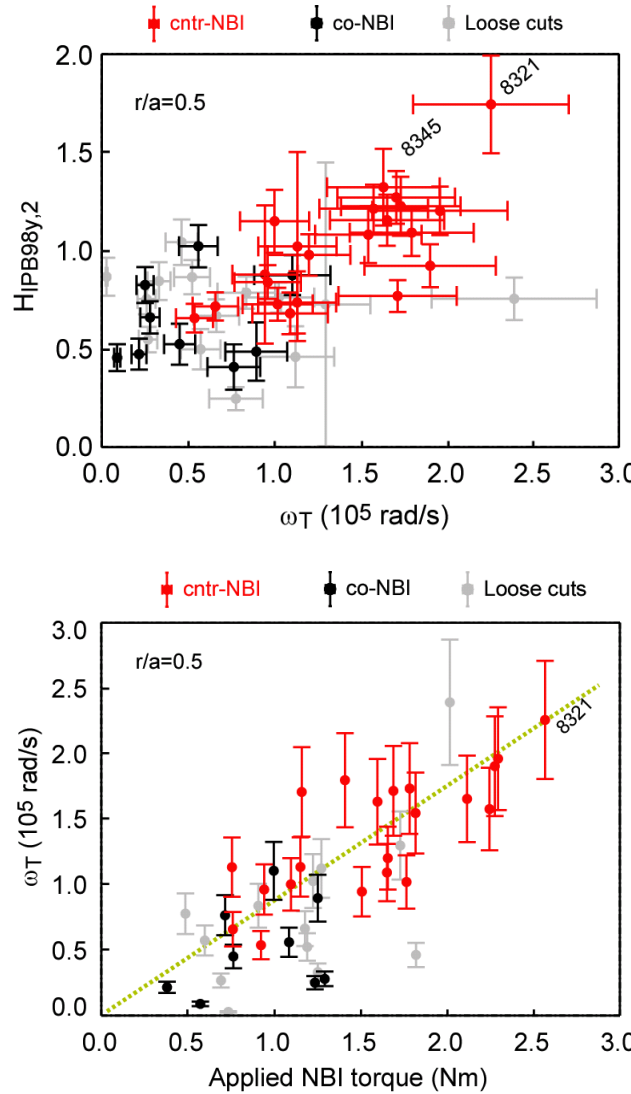


Normalised confinement
across range of L-mode, H-mode and ITB discharges
increases with v_ϕ

v_ϕ driven by torque from the neutral beam. Highest torque in counter-NBI discharges due to asymmetric (co-counter) fast ion losses



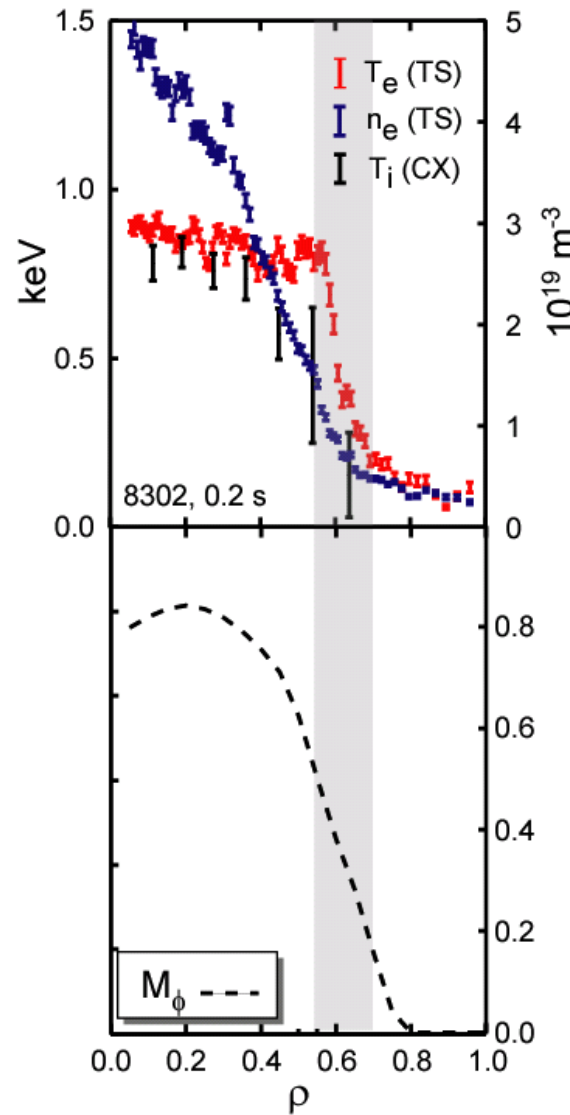
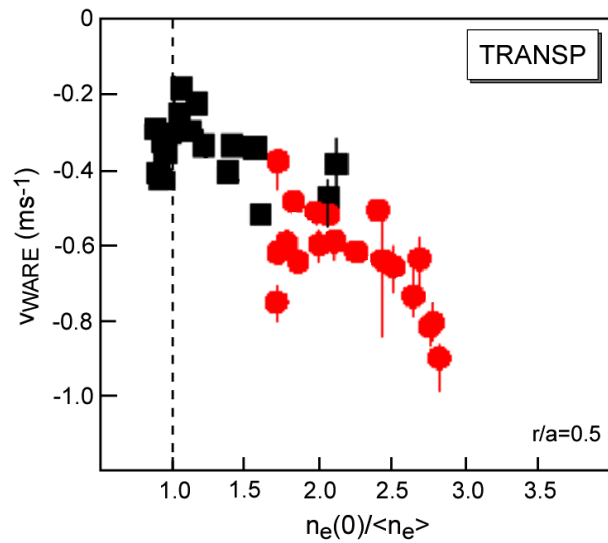
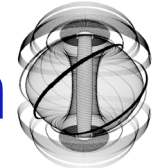
Highest confinement at largest v_ϕ



Highest confinement discharges are **ITB formed with counter-NBI**
 M_ϕ approaches 1 in core
 Very steep electron temperature gradient at $\rho \sim 0.6$
 Very peaked density profile

See R. Akers EX/4-4

Density peaking dominated by Ware pinch



Highest confinement
discharges are **ITB**
formed with counter-NBI

M_ϕ approaches 1 in core
Very steep electron
temperature gradient at
 $\rho \sim 0.6$

Very peaked density
profile

Dominated by Ware
pinch, supplemented by
neutral beam current drive
term

See R. Akers EX/4-4

Flow shear exceeds ITG growth rate



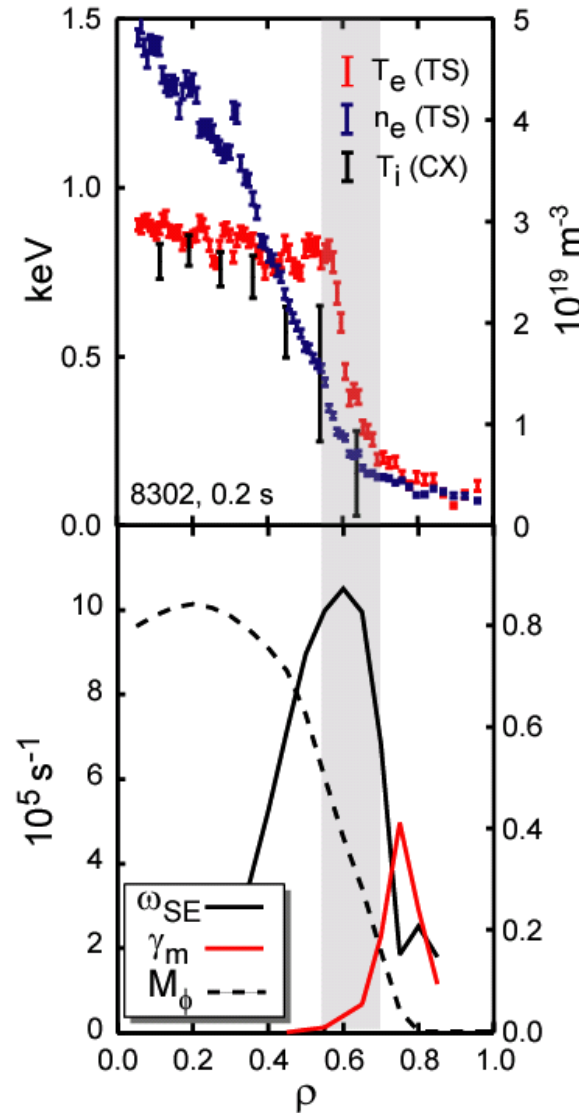
TRANSP estimate of ω_{se} dominates ITG growth rate γ_m

γ_m derived from a simple model, validated against GS2

ω_{se} comparable with estimates of the *ETG* growth rate from GS2 ⇒ **ETG drive stabilisation may be a possibility**

2 surprises:

- flat T_e profile inside ITB
- no clearly diagnosed T_i barrier

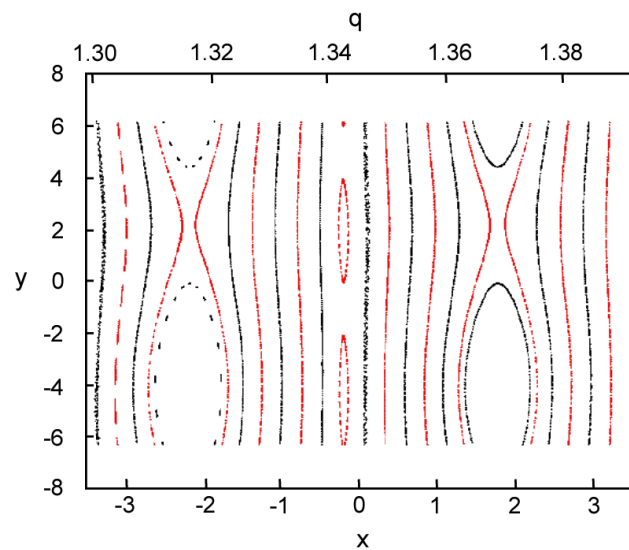
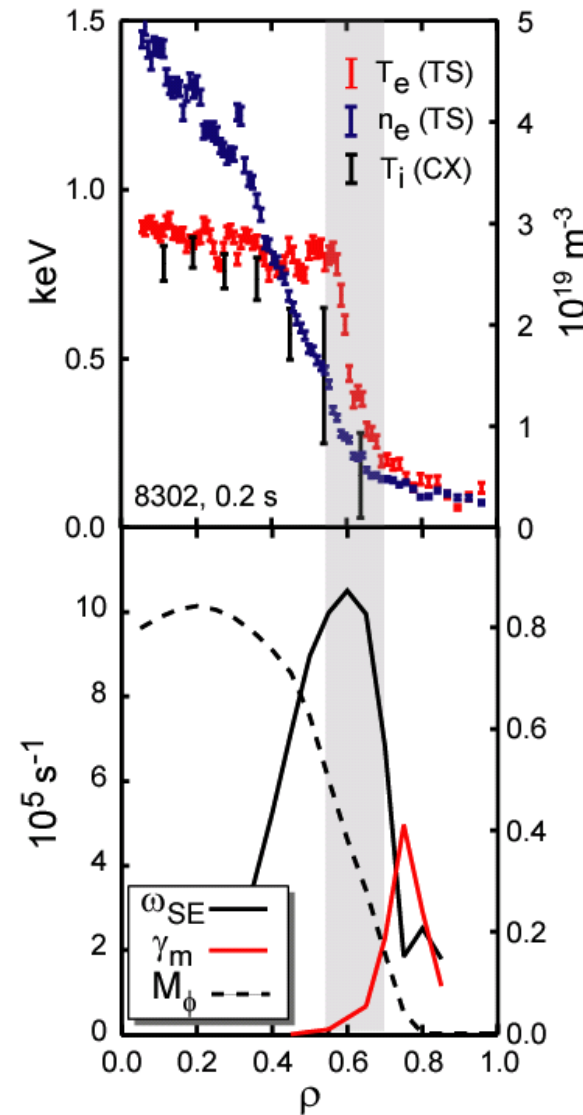




Tearing parity modes unstable in core

Flat T_e profile inside ITB
may be explained by
micro-tearing modes

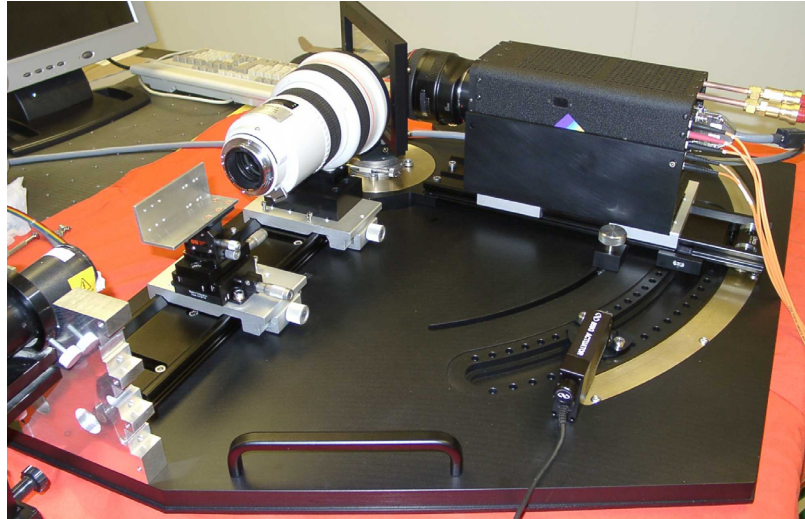
**Tearing parity modes
demonstrated unstable**
on $\psi_N \sim 0.4$ in GS2 runs
with EM effects turned
on



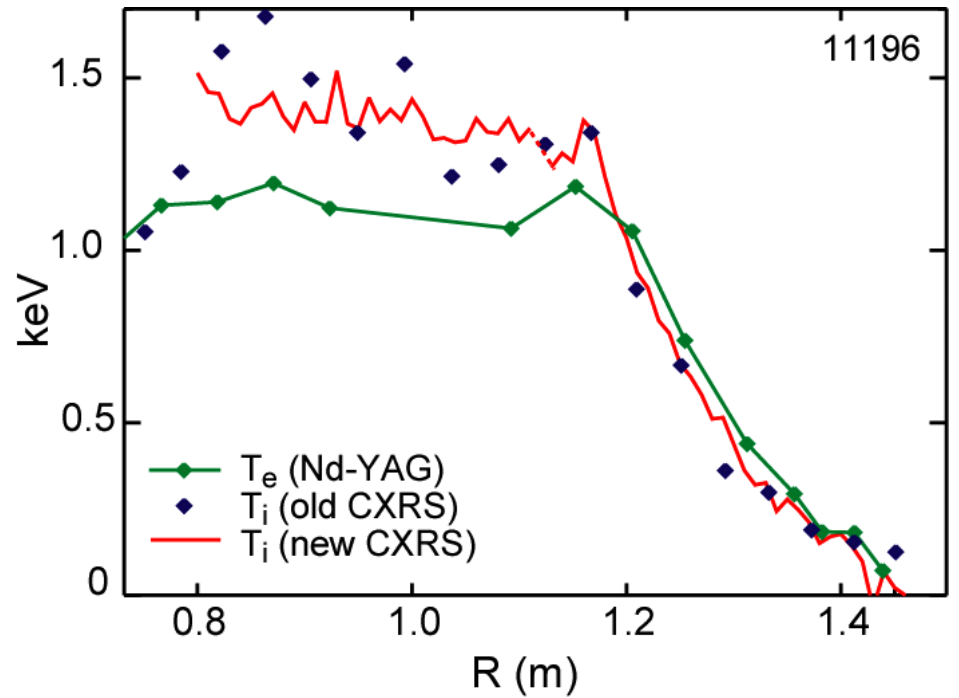
Small islands on high
order rational
surfaces 25/19, 26/19
and secondary
islands between them



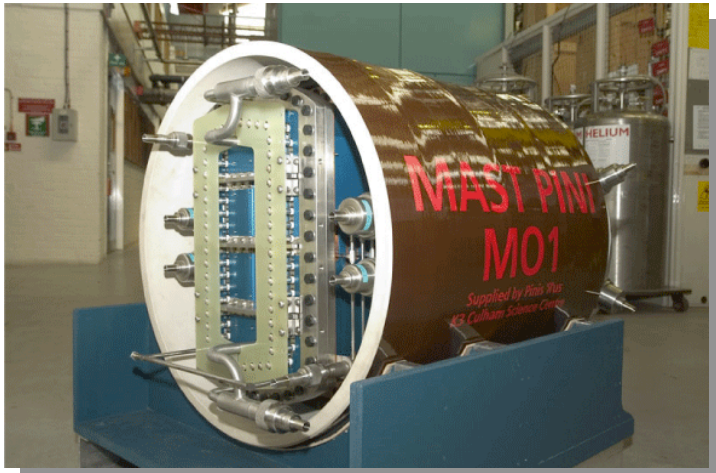
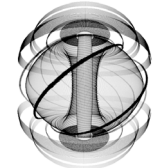
Enhanced T_i spatial resolution required



Upgraded CXRS facilitated by adaptable low A configuration
⇒ 200+ chord spectrometer
spatial resolution $\sim \rho_i$
poloidal and toroidal chords
separate views of two NBI beams



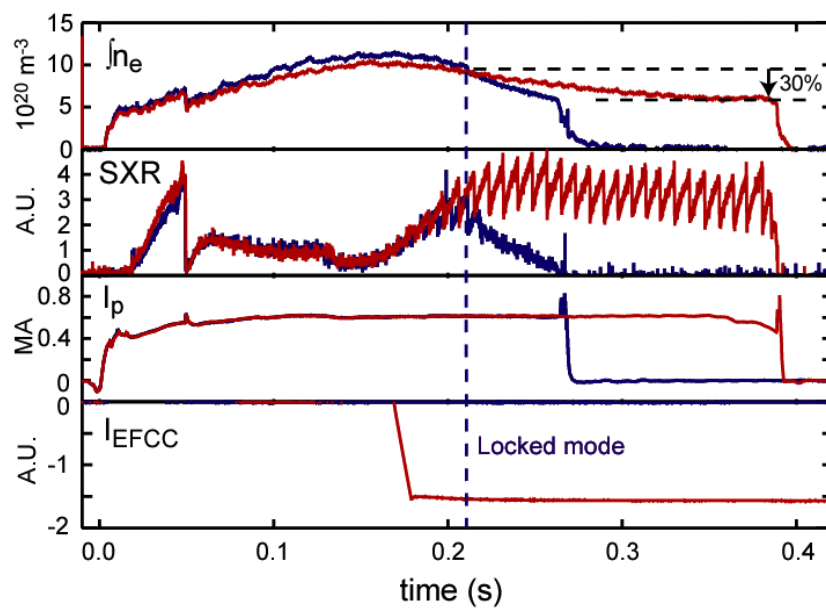
v_ϕ studied with future higher P_{NBI} , longer pulse



High rotation with modest beam power makes MAST ideal for rotation studies (a result of good momentum confinement but low moment of inertia)

Beam upgrade to JET-style PINIs ongoing - ~double P_{NBI} available in most recent campaign

v_ϕ studied with future higher P_{NBI} , longer pulse



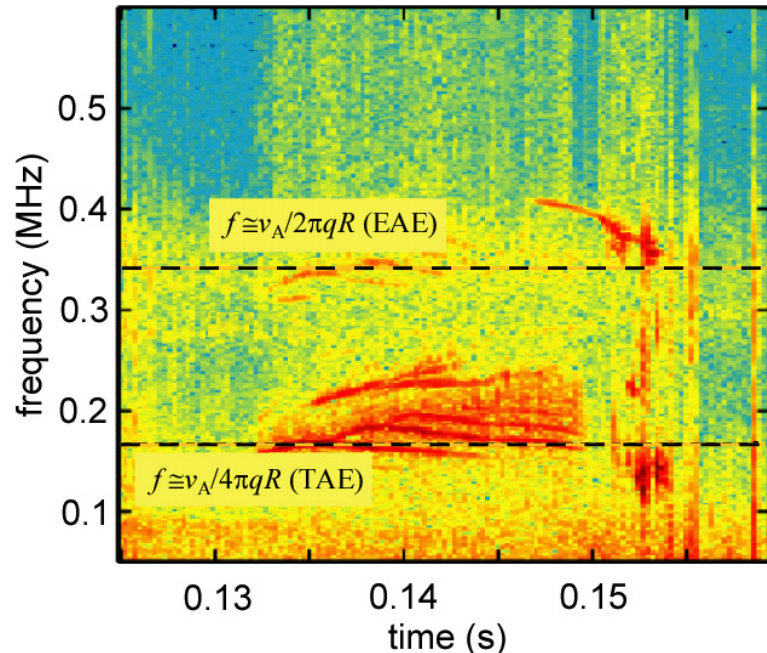
High rotation with modest beam power makes MAST ideal for rotation studies (a result of good momentum confinement but low moment of inertia)

Beam upgrade to JET-style PINIs ongoing - ~double P_{NBI} available in most recent campaign

Increased beam power together with newly installed Error Field Correction coils should give long pulses with high rotation and large fast ion component

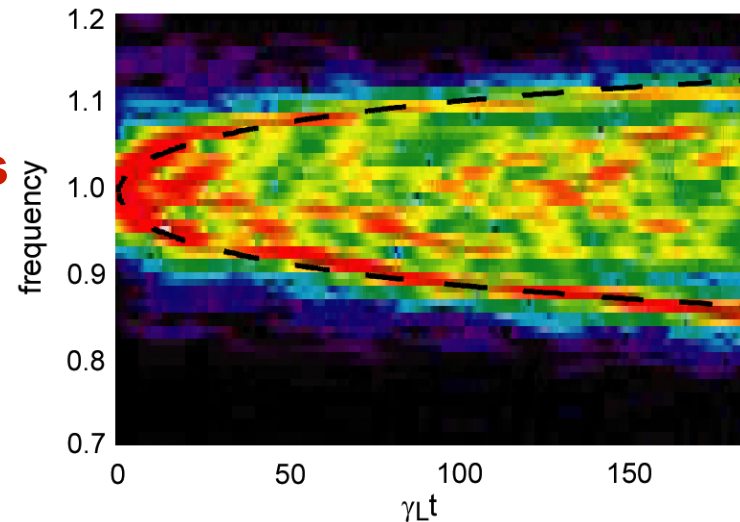
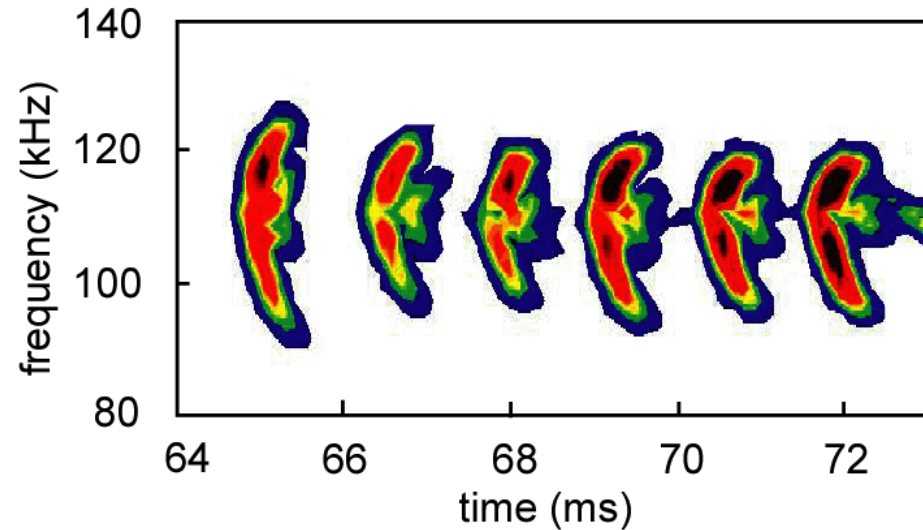
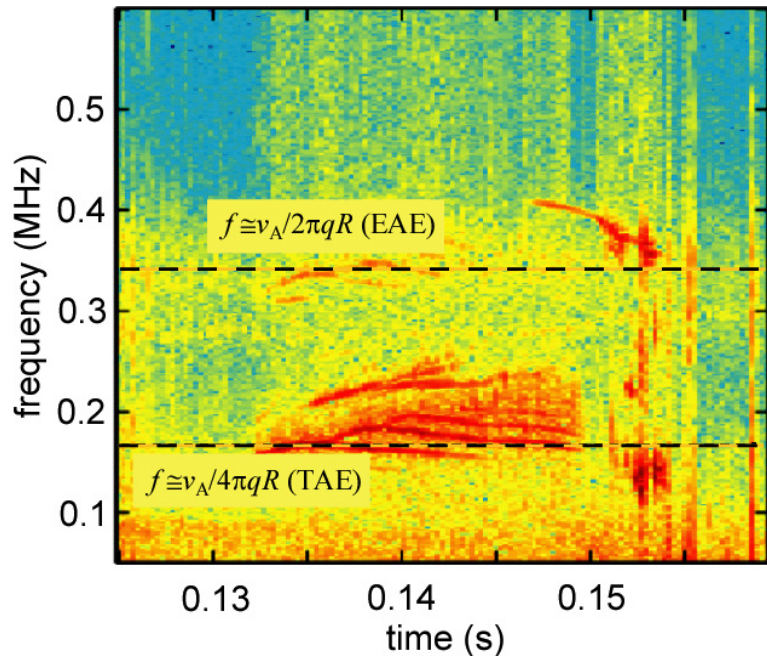


Energetic particle modes explored



Future **large fast ion component and super-Alfvénic beam** ($v_{\parallel, NBI} \sim 0.7 v_{NBI} \sim v_A$) suggest EPMS may be significant
TAE and EAE activity both observed

Frequency sweeping modes observed



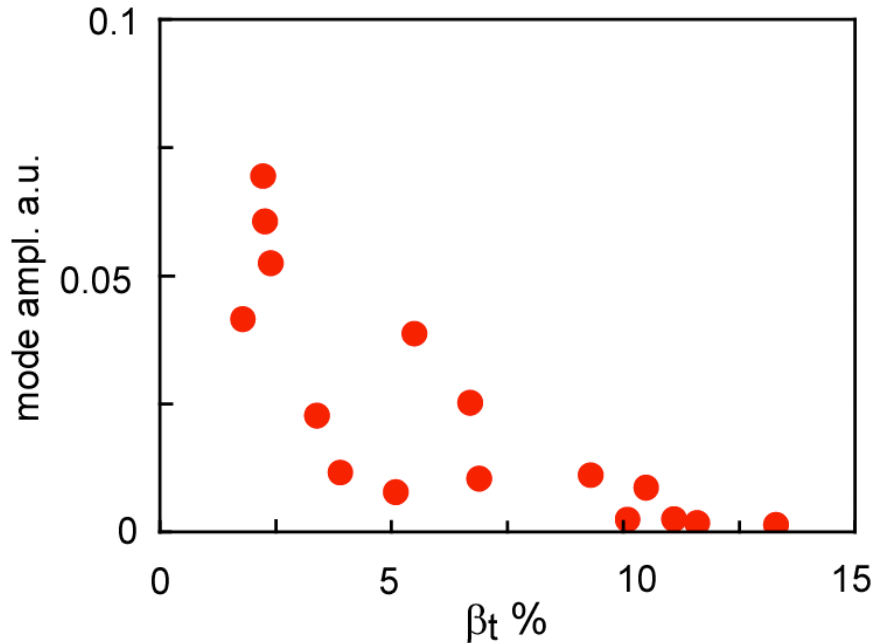
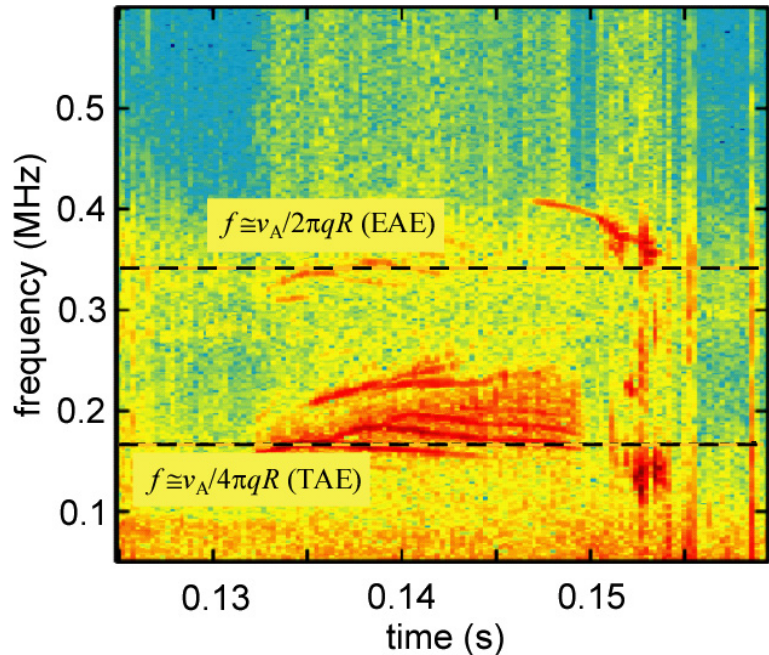
Up-down frequency sweeping modes also observed

Supports model for non-linear evolution of TAE's in the 'explosive' regime - predicts formation of Bernstein-Green-Krushal non-linear waves

Well modelled by HAGIS MHD code



EPM activity reduces with β



For $\beta > 5\%$ TAE and EAE activity become dominated by non perturbative down-frequency chirping modes

The **amplitude of these modes falls sharply with increasing β** , vanishing for $\beta > 15\%$

⇒ AE activity likely to be absent in a future ST device where β on axis would approach 100%

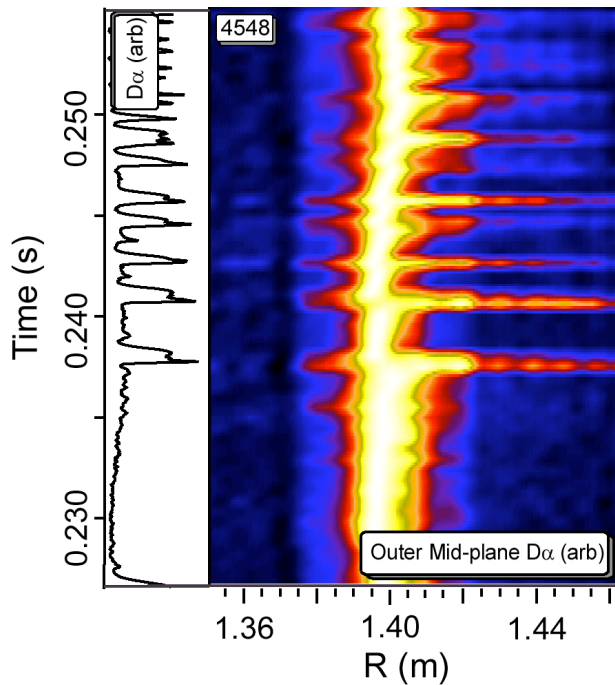
See S. Sharapov EX/5-2Ra



-
- The L-H transition and H-mode Pedestal
 - Confinement and Transport
 - **Transients - ELMs** and Disruptions
 - Start-up without a central solenoid



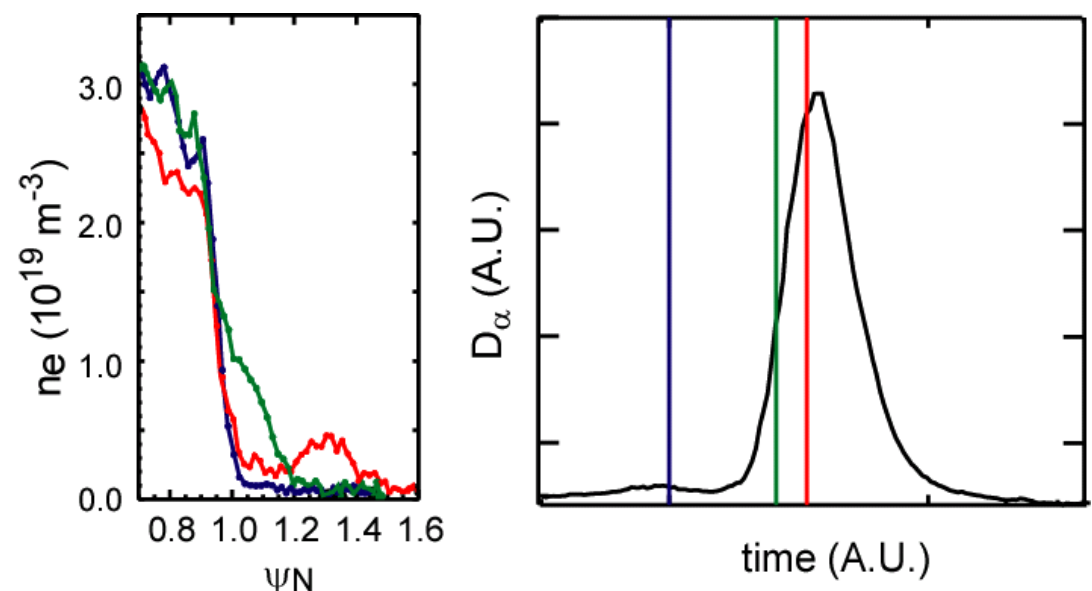
ELM structure exploration continues



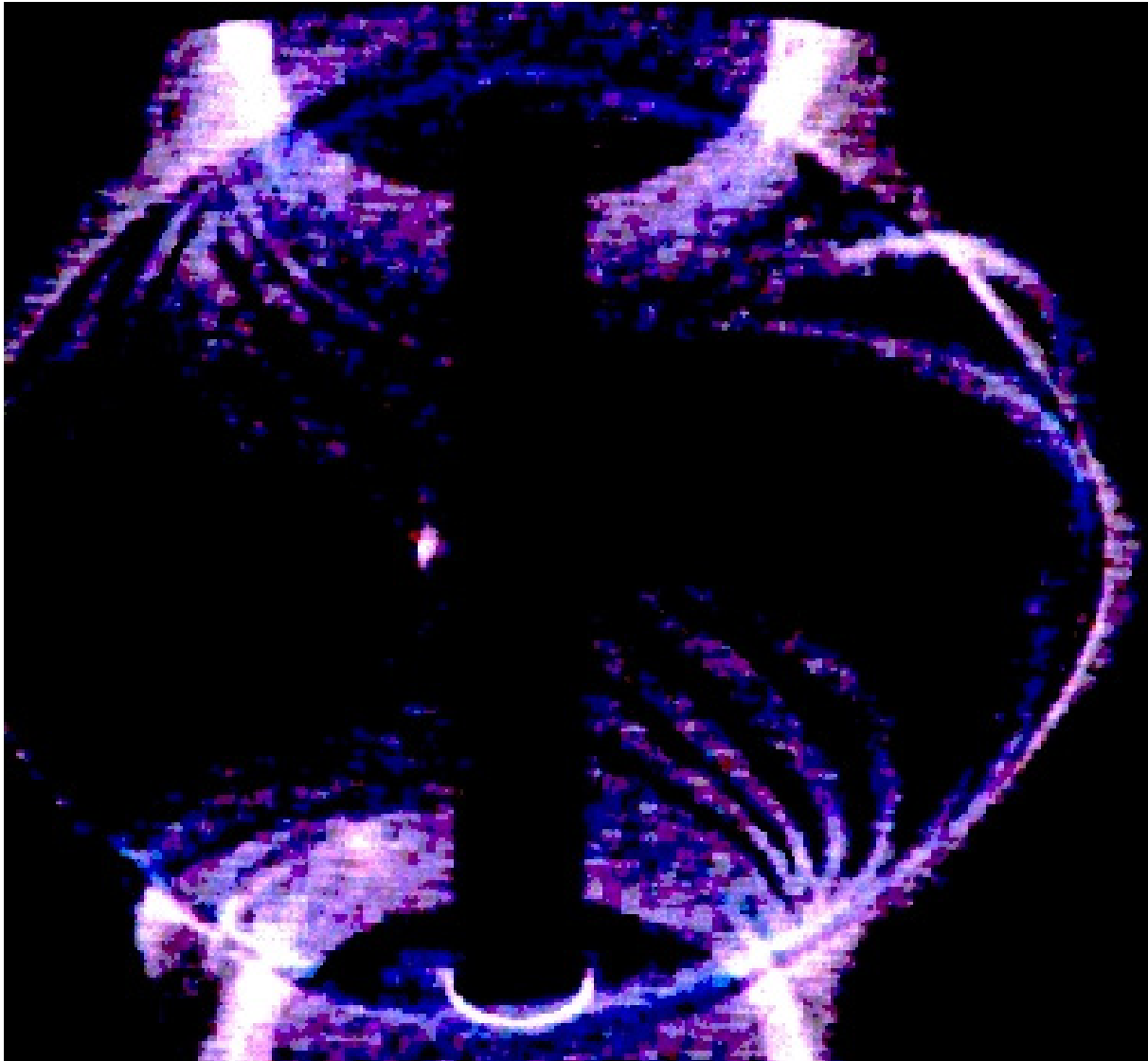
.... and edge density profile
(using high spatial resolution
TS system)

TS profiles also show
formation of 'disconnected'
feature, late in ELM

Previously presented observations of
'radial bursts' during edge localised modes
Visible in edge D_α profile ...



2D fast camera reveals ELM filaments



New 2D visible light images on whole plasma clearly show ELM bursts are, in fact, **filaments**

Toroidal mode number of filaments in the range
 $8 < n < 14$

Filaments appear to push out beyond separatrix, following field lines with $4 < q < 6$

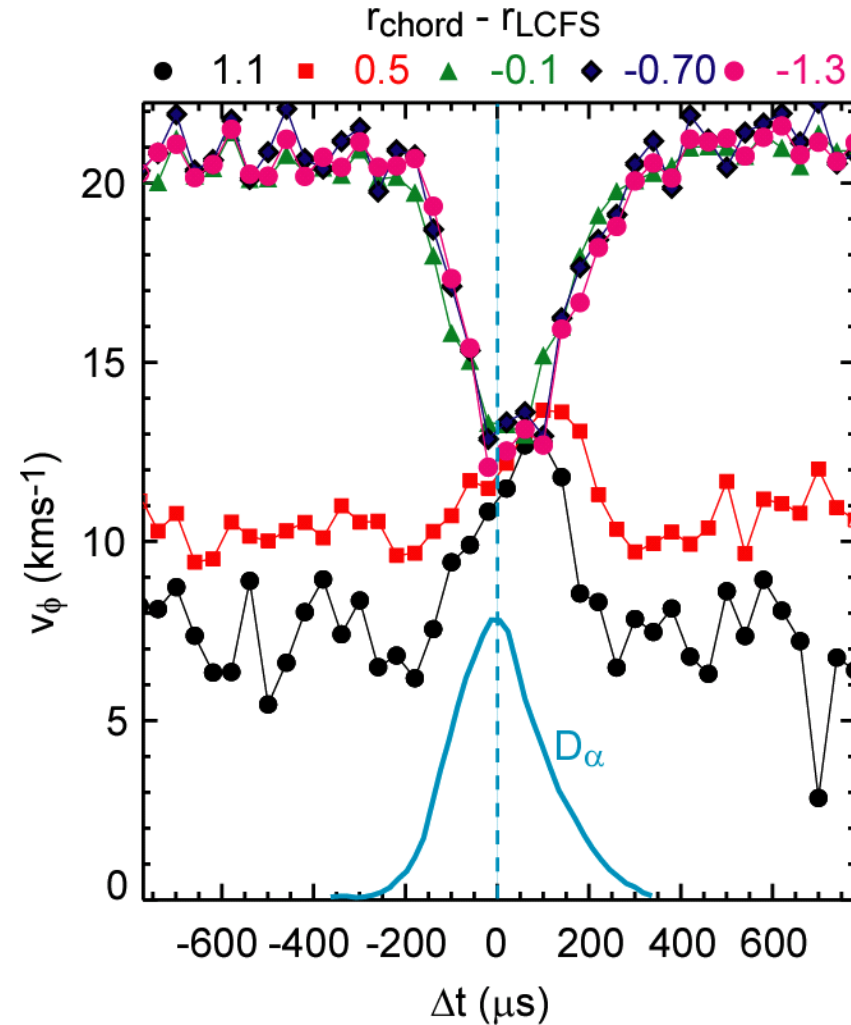


Edge velocity shear disappears at ELM

Fast edge toroidal velocity measurements assembled from He Doppler diagnostic for similar ELMs

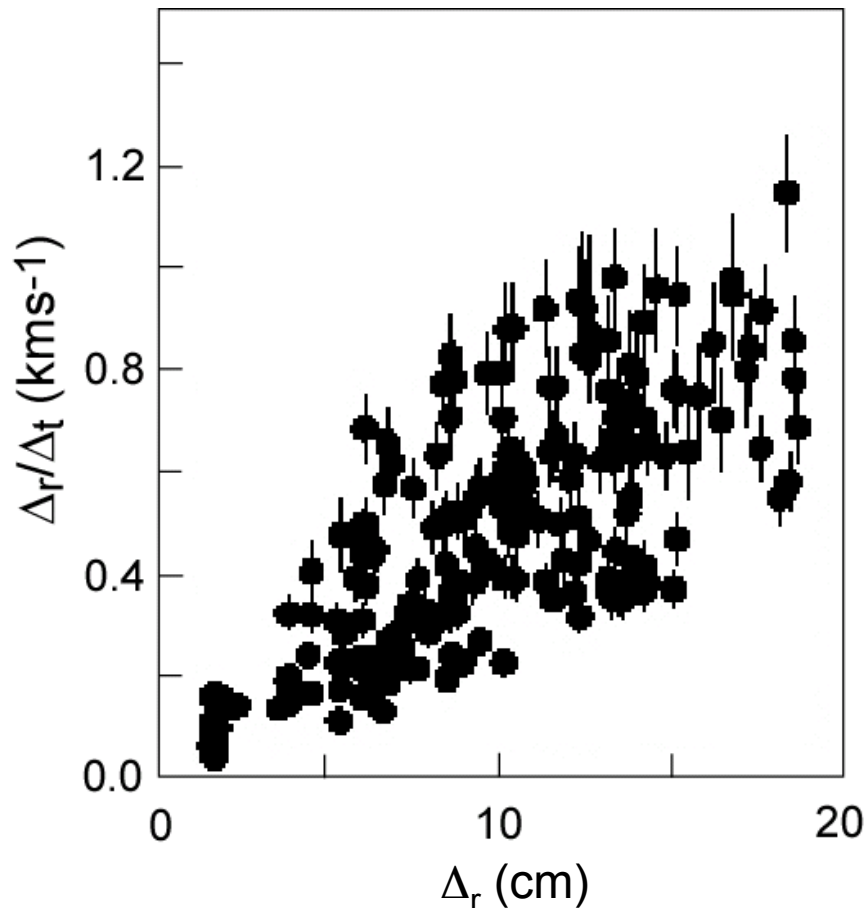
Strong edge **toroidal velocity shear** ($1.8 \times 10^6 \text{ s}^{-1}$) **vanishes around time of ELM** (also observed on COMPASS-D)

May explain how ELM filament can protrude beyond separatrix without being destroyed





Average filament v_r up to $\sim 1\text{km/s}$

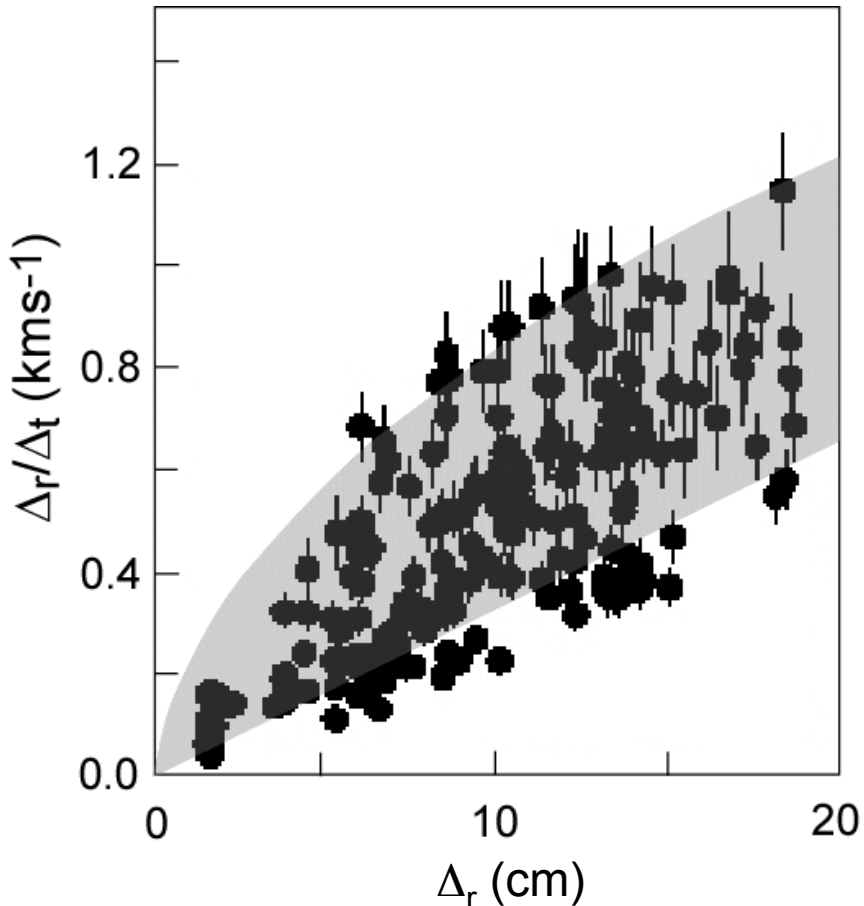


Average radial velocity of ELM filament varies with distance from separatrix (measured by time for interaction with mid-plane reciprocating probe)

See A. Kirk EX/2-3



Filaments are actually accelerating



Average radial velocity of ELM filament varies with distance from separatrix (measured by time for interaction with mid-plane reciprocating probe)

Modelling of data from toroidally separated RPs on MAST indicates:

- ELM filaments are, in fact,
accelerating away from separatrix at $5-15 \times 10^6$ ms⁻²
 - Rotating with the measured edge v_ϕ
- Observations consistent with ELM description as non-linear expansion of intermediate-n ballooning mode

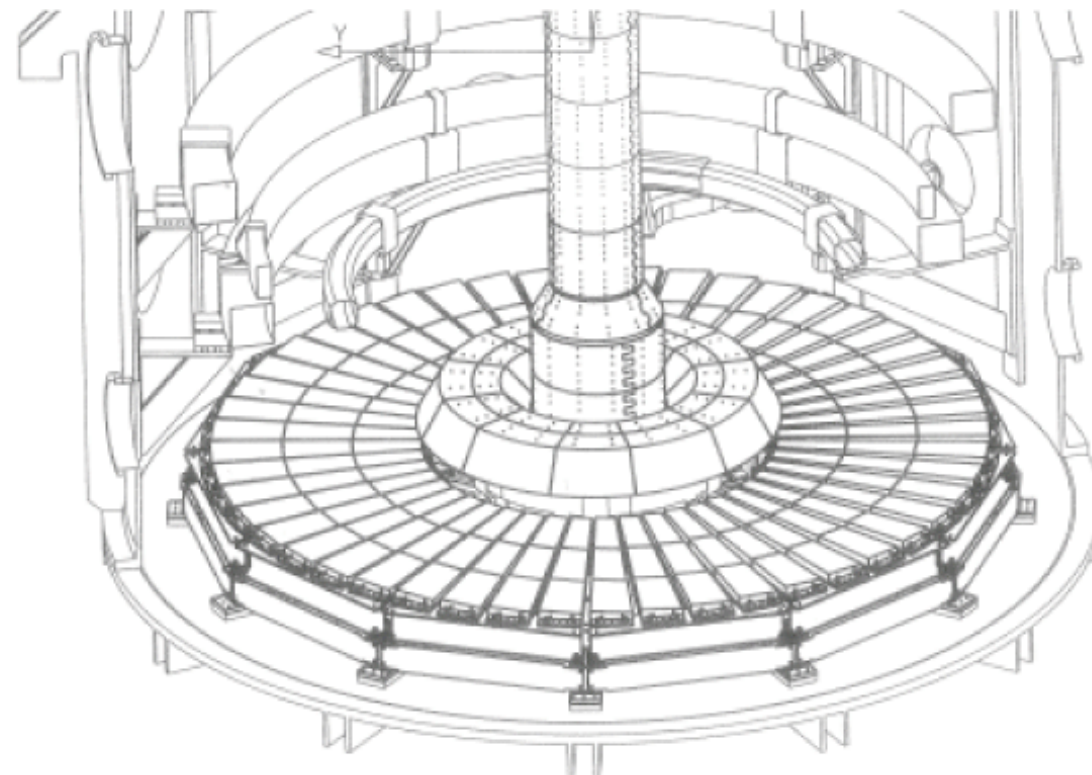
See A. Kirk EX/2-3, H.R. Wilson TH/P1-5



-
- The L-H transition and H-mode Pedestal
 - Confinement and Transport
 - **Transients - ELMs and Disruptions**
 - Start-up without a central solenoid



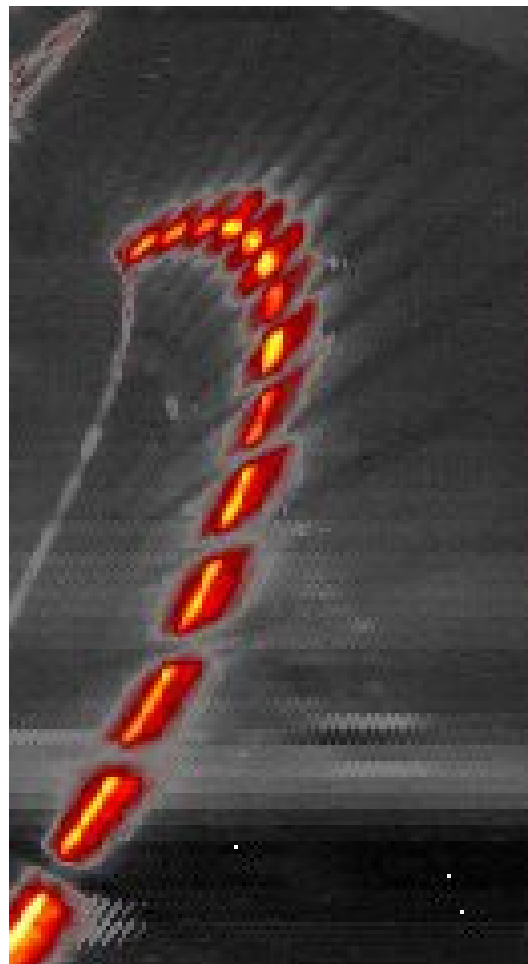
Improved views with new divertor



Disruptions are complex in space and time



Well before disruption

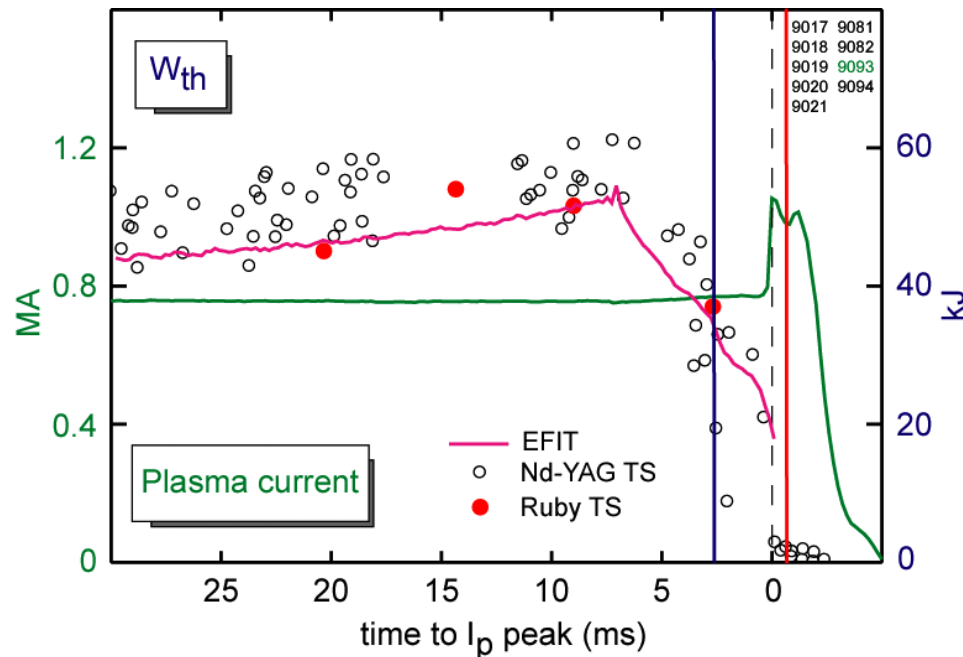


Few ms before
current redistribution



Before current quench

Δ_H broadening reduces peak power loading

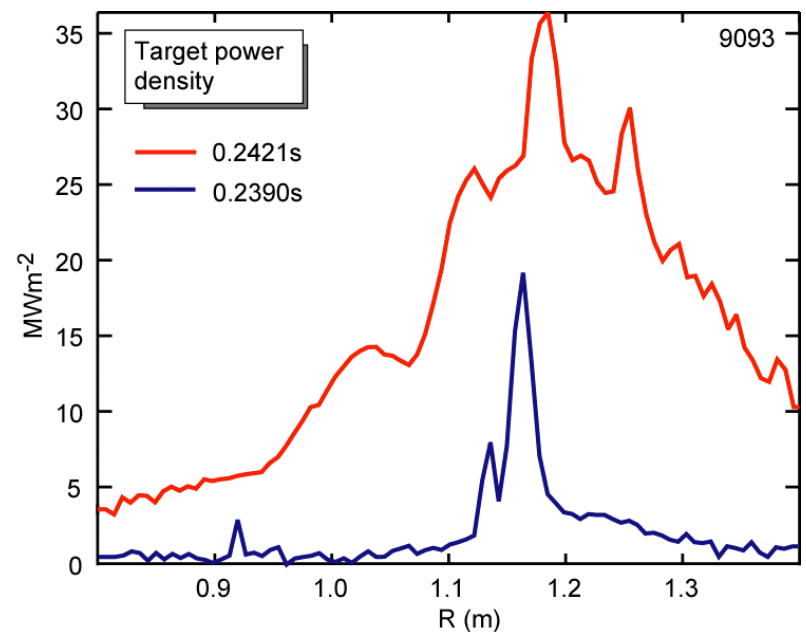


Divertor **power loading rises by factor 2-10** (depending on disruption type) **several ms before current redistribution**

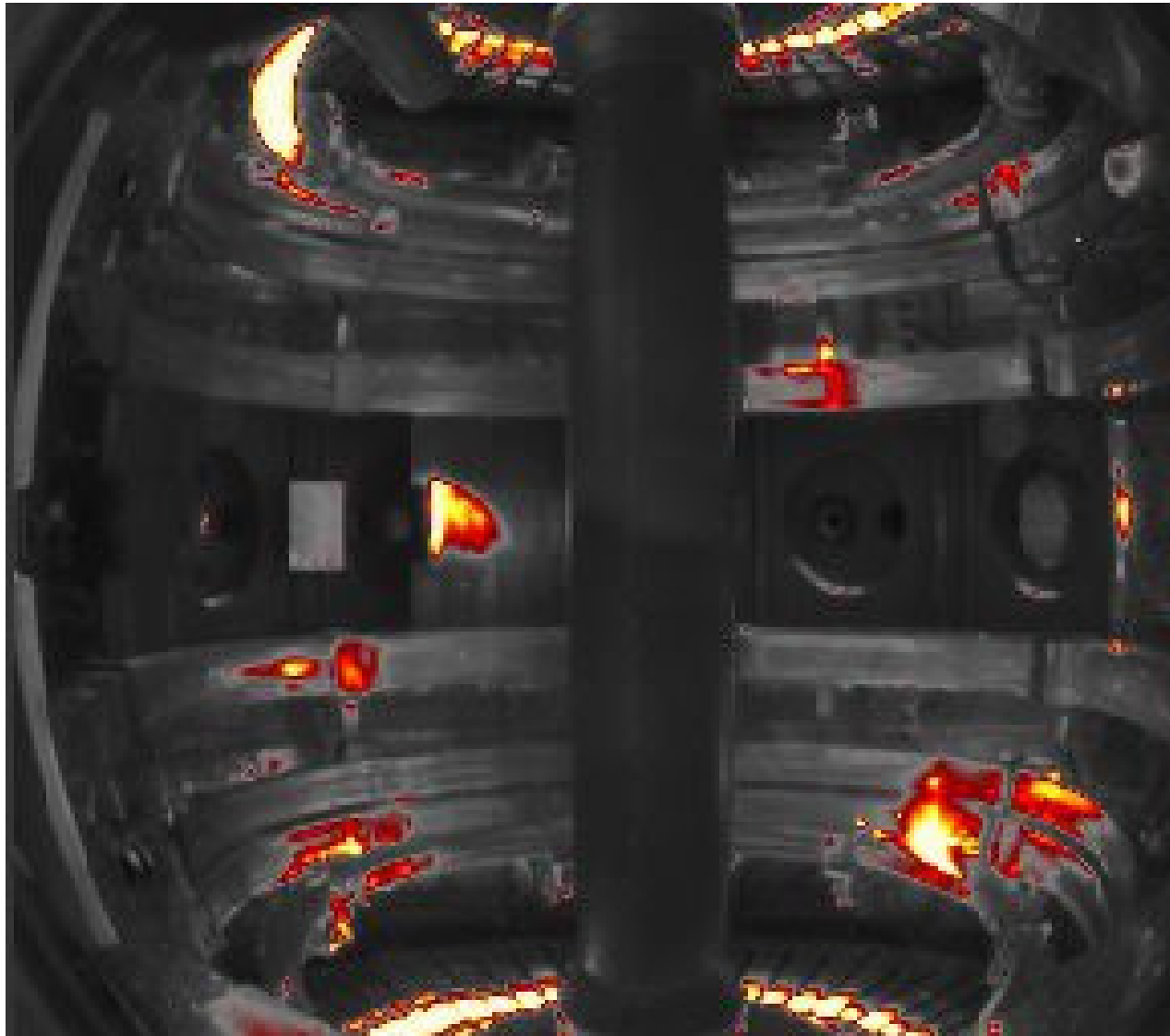
Result of 30-40% of W_{th} losses

Power loading rises by a further factor ~ 2 during current redistribution due to rapid loss (1-2ms) or remaining W_{th}

Power loading is, however, significantly ameliorated by **factor ~ 8 broadening of heat flux width**



Wide-angle IR views reveal wall loads



MAST IR camera can view around 70% of the vessel

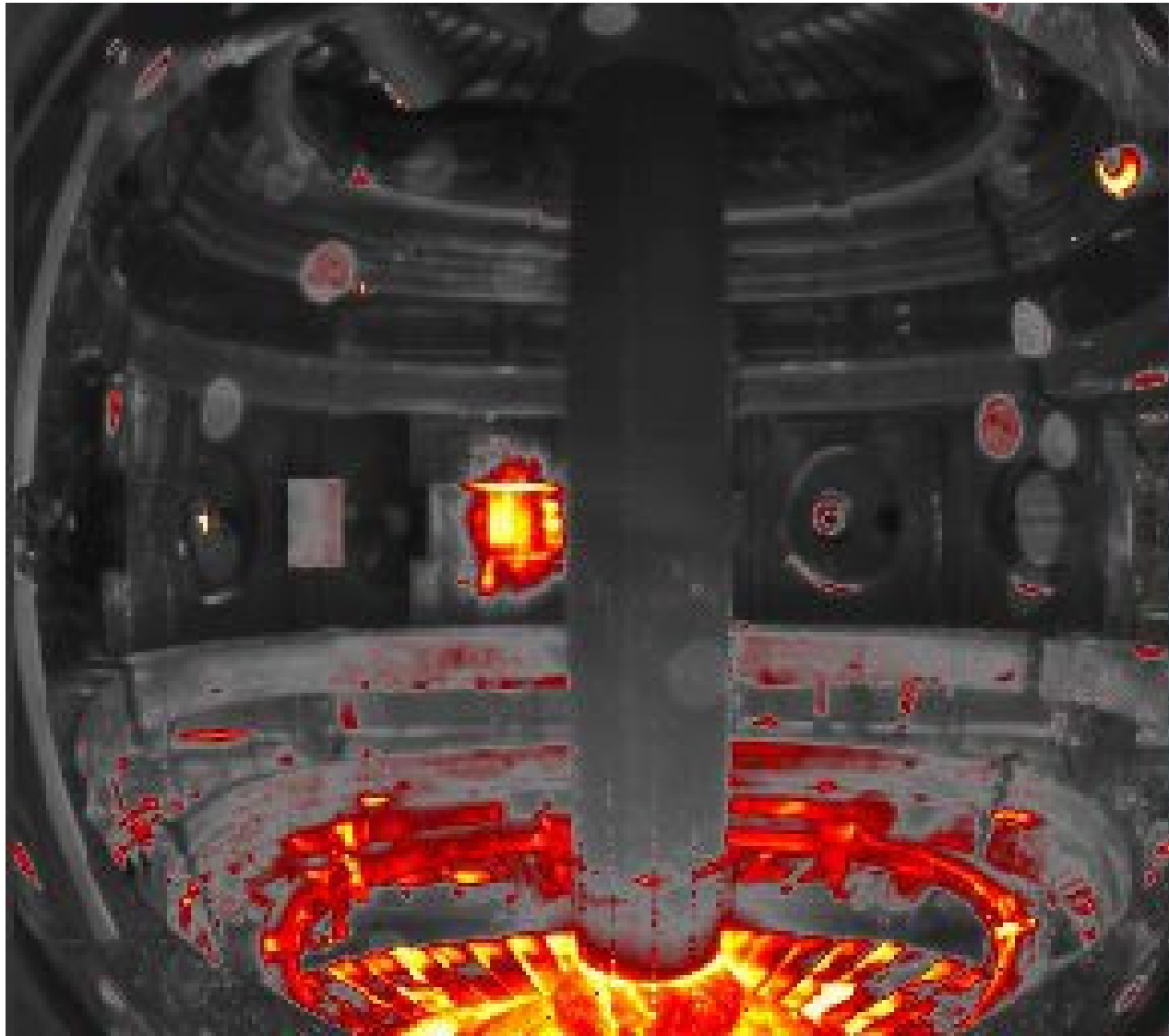
Provides **unique data on first wall interactions and power loading asymmetries**

For example, early phase of disruptions often show $n=1$ wall interaction

Also shows W_{th} losses ~evenly distributed between targets



Toroidal non-uniformity clearly visible



MAST IR camera can view around 70% of the vessel

Provides **unique data on first wall interactions and power loading asymmetries**

Later phase of this VDE disruption show all remaining W_{th} going to lower target

Note the substantial toroidal asymmetry in the target power load



-
- The L-H transition and H-mode Pedestal
 - Confinement and Transport
 - Transients - ELMs and Disruptions
 - Start-up without a central solenoid



Future ST's may not have central solenoid



ST design allows excellent access to the centre column

Even complete replacement for upgrade or repair is relatively straightforward

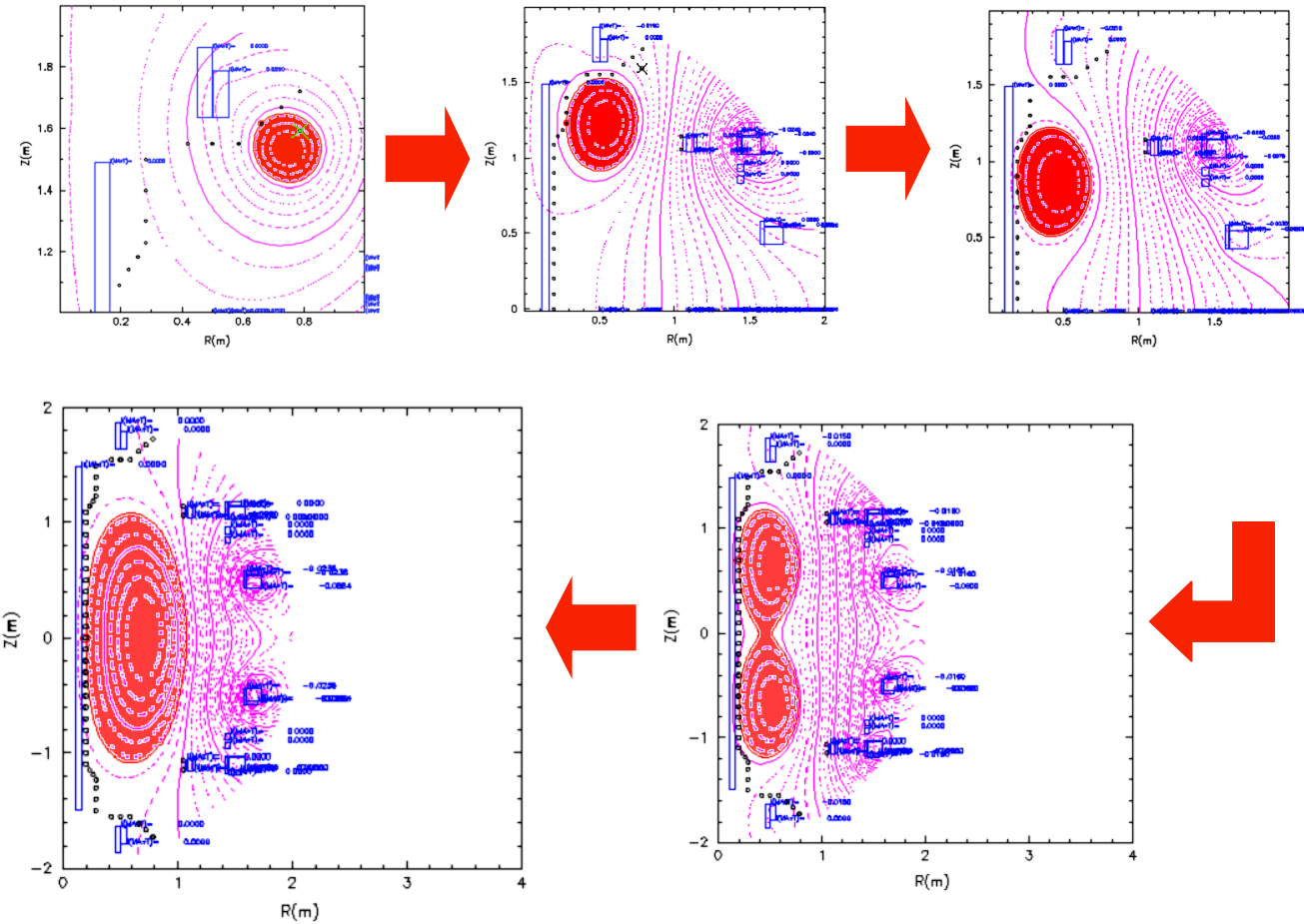
Future ST devices operating with a DT mix, however may not have space for central solenoid due to need for neutron shielding

Alternative schemes for plasma start-up are therefore an important issue for the ST



Alternative start-up schemes investigated

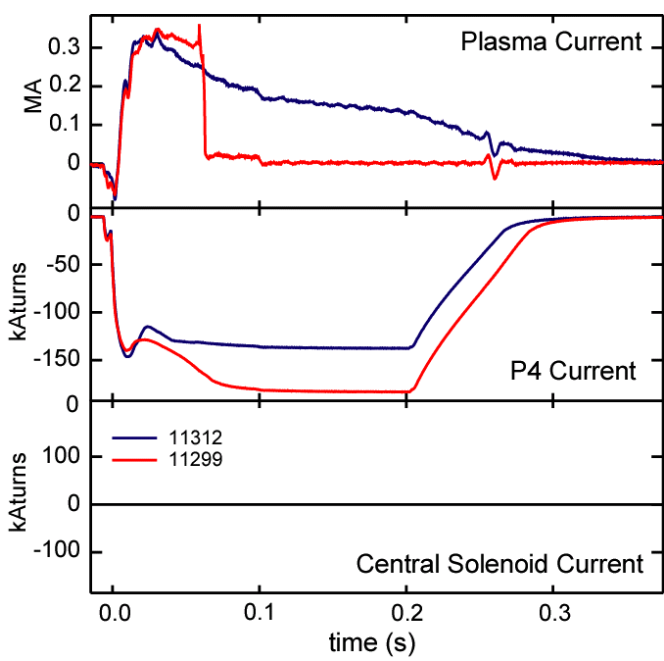
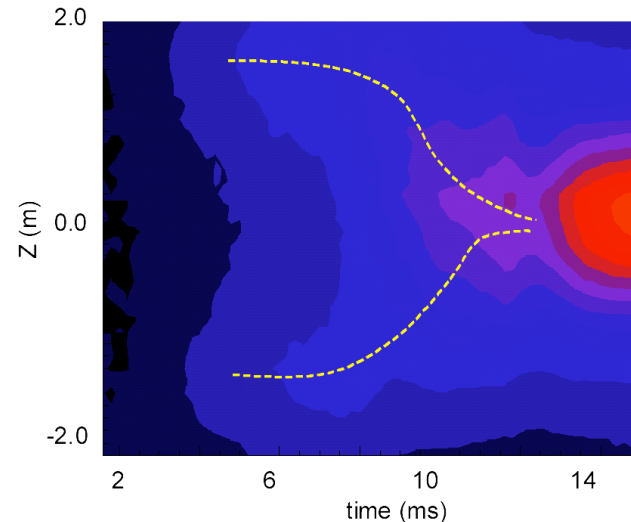
One such scheme is being developed in association with ENEA
Double-null merging (DNM) involves **breakdown at a quadrupole null** between pairs of poloidal coils in upper and lower divertor
Modelling predicts **merging of plasma rings** as current in coils ramped to zero
DNM is compatible with future ST design



340kA target plasma obtained with DNM



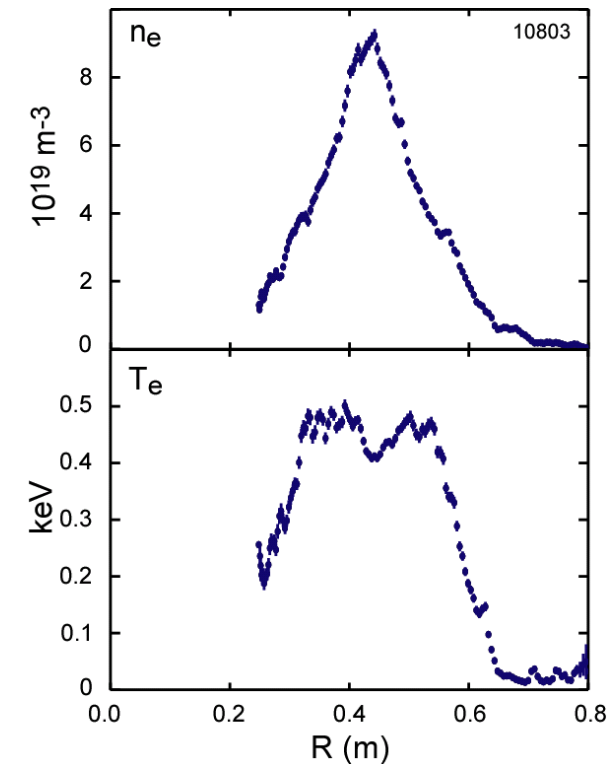
Plasma ring formation
and merging clearly
seen on centre column
magnetic array



So far, **over 340kA**
driven for >50ms,
sustained by B_v ramp

Hot (0.5keV), dense
($9 \times 10^{19} \text{ m}^{-3}$) plasma

Good target for NBI or
RF current drive and
heating

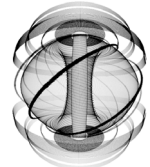




Conclusions

- Exact double-null geometry and high resolution edge diagnostics allow study of physics close to CDND, such as lowering of P_{L-H} (now seen on other devices). Effect of CDND mostly on E_r .
- Addition of large ϵ and high β data (with conventional 'D' shape) to international database improves confidence in scalings and allows better exploration ϵ dependencies.
- Normalised confinement linked to toroidal rotation, driven by neutral beam torque
- TRANSP and GS2 now implemented. v_ϕ dominates ω_{se} , stabilising ITG (and possibly ETG) modes. χ_i at neo-classical levels. Well converged non-linear micro-stability calculations give χ_e of same order as TRANSP.
- Super-Alfvénic fast ions (from neutral beam) generate variety of Alfvén Eigenmode activity, including frequency sweeping modes. TAE/EAE activity falls with increasing β .
- ELMs appear as filamentary structures following perturbed field lines. Rotate with edge plasma, push out beyond separatrix (through region of low velocity shear) and accelerate radially outwards
- Heat flux width broadening (factor ~8) during disruptions reduces peak power loading but significant ω_{th} losses can take place before broadening occurs.
- Double-null merging scheme developed for plasma start-up without central solenoid. Hot, dense tokamak plasma formed with 340kA driven for >50ms

MAST related presentations at 20th IAEA FEC



A Kirk "The structure of ELMs and the distribution of transient power loads in MAST" EX/2-3 Tuesday

RJ Akers "Comparison of plasma performance and transport between tangential co- and counter-NBI heated MAST discharges" EX/4-4 Wednesday

SE Sharapov "Experimental studies of instabilities and confinement of energetic particles on JET and on MAST" EX/5-2Ra Thursday

HR Wilson "The Spherical Tokamak as a Components Test Facility" FT/3-1Ra Friday

M Valovic "Energy and Particle Confinement in MAST" EX/P6-30 Friday

H Meyer "H-mode transition physics close to double null on MAST and its applications to other tokamaks" EX/P3-8 Thursday

AR Field "Core Heat Transport in the MAST Spherical Tokamak" EX/P2-11 Wednesday

H.R. Wilson "Theory of plasma eruptions" TH/P1-5 Wednesday